

POLITECNICO DI TORINO

Master's Degree in BIOMEDICAL ENGINEERING



Master's Degree Thesis

**UVC and blue light-based treatments for
inactivation of bacteria**

Supervisor

Prof. Guido PERRONE

Candidate

Giulia PALMA

December 2021

Summary

Disinfection using the short-wavelength Ultra-Violet (the UVC, 200-280 nm) has been known for over a century but is gaining increasing popularity in these years thanks to the combined effect of the COVID19 pandemic outbreak, the stronger emerging of antibiotic resistant bacteria, and the availability of new compact LED sources in replacement for the traditional mercury vapor lamps, which are being banned for their toxic mercury content. UVC irradiation can be exploited both for its direct damaging action on the bacteria RNA or DNA and for its indirect mechanism, the so-called Photo-Dynamic Therapy (PDT), in which it triggers the generation of cytotoxic Reactive Oxygen Species (ROSs) from a non-toxic photosensitizer (PS). Long-term UVC exposure, however, can also be dangerous and have carcinogenic effects on human cells; an alternative is represented by the generation of ROSs from suitable photosensitizers that can be excited with the less harmful blue light (400-470 nm).

This thesis focuses on the study of the use of UVC and blue light for sanitization of water. The microbiological safety of water is essential to prevent waterborne diseases, which are one of the leading causes of human deaths, affecting millions of people worldwide. “Clean water and sanitation”, distribution of safe drinking water to everyone and hygiene are the sixth of the *Sustainable Development Goals* of the United Nations.

In the first part of this thesis, the effectiveness of the mechanism of UVC has been studied and some water sanitization solutions have been analyzed. A simplified model of the LED irradiation based on Lambertian sources has been developed and implemented in MATLAB® to analyze various configurations and evaluate the optimal geometry that guarantees a uniform irradiation dose for bacteria inactivation. The developed simulation code has been validated using a commercial ray-tracing software, *TracePro*®. Then, the UVC germicidal action has been experimentally proven with extensive tests on contaminated water at different exposure times, using culture media sensitive to *Enterobacteriaceae*. The results show the relevant antimicrobial UVC effect with exposure times of 1-2 s with a final bacteria concentration lower than 10^3 CFU/mL.

In the second part of the work, the UVC disinfection has been compared against

the effect of blue light plus a suitable photosensitizer. Based on evidences in the literature, curcumin has been chosen as natural photosensitizer because of its extended antimicrobial activity with blue light and its safety evaluated by clinical trials on humans; indeed, it is commonly used in dentistry for oral disinfection. This part has been mainly experimental and different curcumin concentrations and exposure times have been studied. In general, it has been found that longer exposure times are required than when using UVC. This prolonged treatment could lead to an increase of temperature, which could be responsible of part of the antimicrobial action; therefore, to assess the specific efficacy of the PDT and isolate the thermal effect contribution, Pulsed Wave (PW) irradiation has been used, while measuring the induced temperature with Fibre Bragg Grating (FBG) sensors.

Keywords: *UVC, Antimicrobial, Water Disinfection, Lambertian Source, Dose, Enterobacteriaceae, Photo-Dynamic Therapy, Blue Light Therapy, Photosensitizer, Curcumin, Temperature, Fibre Bragg Grating.*

*To my Brother, my Father and my Mother,
with all my Love.*

Table of Contents

List of Tables	IX
List of Figures	X
Acronyms	XV
1 Objectives, overview and structure of the thesis	1
2 Introduction	3
2.1 Introduction to Radiation	5
2.1.1 General parameters involved	6
2.2 Mechanism of disinfection with Radiation	7
3 Water Disinfection with UVC	10
3.1 Ultra-Violet C (UVC)	11
3.1.1 Operating principle	11
3.1.2 UVC-light for COVID-19	13
3.2 Introduction to Light Emitting Diodes	13
3.3 UVC-Light emitting diodes	16
3.3.1 Low pressure ultraviolet (LPUV)	16
3.3.2 UVC-LEDs	16
3.3.3 Comparison between UVC-LEDs and LPUV	18
3.3.4 UVC-LEDs Limits	19
3.3.5 State of the art	19
3.4 Continuous Wave (CW) and Pulsed light (PL) modes	20
4 Water Disinfection with PDT and Blue light	22
4.1 Photodynamic Therapy (PDT)	22
4.1.1 Operating principle	23
4.1.2 Photosensitizers	23
4.2 Blue-light	24

4.2.1	Operating Principle	24
4.2.2	State of the art	25
4.3	Continuous Wave (CW) and Pulsed Light (PL) modes	25
5	Simulation of LED-based sources	27
5.1	LED simulation	27
5.1.1	Lambertian source	28
5.2	Single source on a plane	30
5.2.1	CASE 1a	30
5.2.2	Validation	33
5.3	Different sources on a plane	36
5.3.1	CASE 2a	36
5.3.2	CASE 3a	38
5.3.3	CASE 4a	40
5.3.4	CASE 5a	42
5.3.5	Comparison of the 5 CASES a	44
5.4	Different sources on two parallel planes	46
5.4.1	CASE 1b	47
5.4.2	CASE 2b	48
5.4.3	CASE 3b	49
5.4.4	CASE 4b	50
5.4.5	CASE 5b	51
5.4.6	Comparison of the 5 CASES b	52
5.5	Aluminum Structure	54
5.5.1	Discussion	55
6	Experimental Section 1: UVC and blue LEDs for water disinfection	57
6.1	Circuit: UVC and blue LED	57
6.1.1	Material & Methods	58
6.1.2	First set of tests	60
6.1.3	Second set of tests	62
6.1.4	Third set of tests	63
6.1.5	Discussion	63
6.2	Experimental Section 2: UVC-LEDs in aluminum tube	64
6.2.1	Material & Methods	66
6.2.2	First set of tests	67
6.2.3	Second set of tests	68
6.2.4	Discussion	69
6.3	Evaluations on Aluminum Tube	70

7	Experimental Section 2 : Blue LED with curcumin for water disinfection	73
7.1	Blue light LED with curcumin on water	73
7.2	Circuit: blue LED	73
7.2.1	Material & Methods	74
7.2.2	First set of tests	75
7.2.3	Second set of tests	79
7.2.4	Discussion	80
8	Conclusions	82
	Bibliography	84

List of Tables

3.1	LPUV lamps vs UVC-LEDs.	19
5.1	Maximum of irradiance at different distances h, Case 1a.	31
5.2	Percentage decrease at each step d, Case 1a.	33
5.3	Maximum of irradiance at different distances h, Case 2a.	38
5.4	Percentage decreases at each step d, Case 2a.	38
5.5	Maximum of irradiance at different distances h, Case 3a.	39
5.6	Percentage decreases at each step d, Case 3a.	40
5.7	Maximum of irradiance at different distances h, Case 4a.	41
5.8	Percentage decreases at each step d, Case 4a.	42
5.9	Maximum of irradiance at different distances h, Case 5a.	43
5.10	Percentage decreases at each step d, Case 5a.	44
5.11	Maximum of irradiance at different distances h, Cases a.	45
5.12	Percentage decreases at each step d, Cases a.	45
5.13	Maximum of irradiance at different distances h, Cases b.	52
5.14	Percentage decreases at each step d, Cases b.	53
5.15	Percentage increases of Cases b after implementation with aluminum reflectance.	56
6.1	Comparisons: $Q_1 = 600 \text{ L/h}$, $d_1 = 1.7 \text{ cm}$	70
6.2	Comparisons: $Q_1 = 600 \text{ L/h}$, $d_2 = 2.5 \text{ cm}$	70
6.3	Comparisons: $Q_1 = 600 \text{ L/h}$, $d_3 = 5.08 \text{ cm}$	71
6.4	Comparisons: $Q_1 = 600 \text{ L/h}$, $d_4 = 7.62 \text{ cm}$	71
6.5	Comparisons: $Q_2 = 2,200 \text{ L/h}$, $d_1 = 1.7 \text{ cm}$	72
6.6	Comparisons: $Q_2 = 2,200 \text{ L/h}$, $d_2 = 2.5 \text{ cm}$	72
6.7	Comparisons: $Q_2 = 2,200 \text{ L/h}$, $d_3 = 5.08 \text{ cm}$	72
6.8	Comparisons: $Q_2 = 2,200 \text{ L/h}$, $d_4 = 7.62 \text{ cm}$	72

List of Figures

2.1	Sustainable Development Goals in 2030.	4
2.2	The electromagnetic spectrum [3].	6
2.3	Mechanisms for cell damage by radiation: direct and indirect effect on DNA.	7
2.4	Direct mechanism for cell damage.	8
3.1	Ultraviolet radiation spectrum.	11
3.2	UVC inactivation mechanism.	12
3.3	Forward-bias for p-n semiconductor junction [15].	15
3.4	Reverse-bias for p-n semiconductor junction [15].	15
3.5	Baloon-shaped irradiation profile [17].	17
3.6	UVC-LED peak at 275 nm and germicidal effectiveness curve [19].	17
3.7	Nominal irradiance of three LEDs compared to the narrow spike of LP lamps (in green, 254 nm), [22].	18
4.1	PDT working mechanism.	23
5.1	Circular source of diameter w , irradiating a plane in which the point X dists h from the source and r from its normal, forming an angle ϕ	29
5.2	Contour plot of the irradiance of the LED at a distance of $h = 1$ cm from the surface, CASE 1a.	30
5.3	Contour plot and Pseudo-color plot of irradiance of the LED at a distance of $h = 1$ cm from the surface, CASE 1a.	31
5.4	Pseudo-color plot of the variation of LED intensity: different distances (h) of the surface and the corresponding maximum of irradiance (E), CASE 1a.	32
5.5	Contour plot of the variation of LED intensity: different distances (h) of the surface and the corresponding maximum of irradiance (E), CASE 1a.	32
5.6	Distance-dependence of 1 LED irradiance, CASE 1a.	33

5.7	Initial model: LED (yellow) on a plane $4 \times 4 \text{ cm}$ and that distant 2 cm from the target surface.	34
5.8	LED-ON distant 1 cm from the target surface.	34
5.9	Parameters set for the LED source.	35
5.10	Irradiance Map: CASE 1a.	35
5.11	Contour plot and pseudo-color representation of irradiance, in a surface with $h = 0.5 \text{ cm}$, with coordinates $P_1(0.5,0)$, $P_2(-0.5,0)$, CASE 2a.	36
5.12	Pseudo-color plot of the variation of LEDs intensity: different distances (d) of the surface and the corresponding maximum of irradiance (E), CASE 2a.	37
5.13	Distance-dependence of 2 LEDs irradiance, CASE 2a.	37
5.14	Contour plot and pseudo-color representation of irradiance, in a surface with $h = 0.5 \text{ cm}$, with coordinates $P_1(-0.75,0)$, $P_2(-0.25,0)$, $P_3(0.25,0)$, $P_4(0.75,0)$, CASE 3a.	38
5.15	Pseudo-color plot of the variation of LEDs intensity: different distances (d) of the surface and the corresponding maximum of irradiance (E), CASE 3a.	39
5.16	Distance-dependence of 4-in-line-LEDs irradiance, CASE 3a.	39
5.17	Contour plot and pseudo-color representation of irradiance, in a surface with $h = 0.5 \text{ cm}$, with coordinates $P_1(-0.5,0.5)$, $P_2(-0.5,-0.5)$, $P_3(0.5,0.5)$, $P_4(0.5,-0.5)$, CASE 4a.	40
5.18	Pseudo-color plot of the variation of LEDs: different distances (d) of the surface and the corresponding maximum of irradiance (E), CASE 4a.	41
5.19	Distance-dependence of 4 LEDs irradiance, square of 1 cm, CASE 4a.	41
5.20	Contour plot and pseudo-color representation of irradiance, in a surface with $h = 0.5 \text{ cm}$, with coordinates $P_1(-0.25,0.25)$, $P_2(-0.25,-0.25)$, $P_3(0.25,0.25)$, $P_4(0.25,-0.25)$, CASE 5a.	42
5.21	Pseudo-color plot of the variation of LEDs: different distances (d) of the surface and the corresponding maximum of irradiance (E), CASE 5a.	43
5.22	Distance-dependence of 4 LEDs irradiance, square of 0.5 cm, CASE 5a.	43
5.23	Comparison of the distance-dependence of irradiance of the treated Cases a.	44
5.24	Comparison between the three exposure times, CASES a.	46
5.25	Pseudo-color plot of the variation of LED intensity: different distances (d) of the surface and the corresponding maximum of irradiance (E), CASE 1b.	47
5.26	Distance-dependence of 1 LED irradiance, CASE 1b	47

5.27	Pseudo-color plot of the variation of LEDs: different distances (d) of the surface and the corresponding maximum of irradiance (E), CASE 2b.	48
5.28	Distance-dependence of 2 LEDs irradiance, CASE 2b.	48
5.29	Pseudo-color plot of the variation of LEDs: different distances (d) of the surface and the corresponding maximum of irradiance (E), CASE 3b.	49
5.30	Distance-dependence of 4-in-line-LEDs irradiance, CASE 3b.	49
5.31	Pseudo-color plot of the variation of LEDs: different distances (d) of the surface and the corresponding maximum of irradiance (E), CASE 4b.	50
5.32	Distance-dependence of 4 LEDs irradiance, square of 1 cm, CASE 4b.	50
5.33	Pseudo-color plot of the variation of LEDs: different distances (d) of the surface and the corresponding maximum of irradiance (E), CASE 5b.	51
5.34	Distance-dependence of 4 LEDs irradiance, square of 0.5 cm, CASE 5b.	51
5.35	Comparison of the distance-dependence of irradiance of the treated Cases b, $\phi_e = 100$ mW.	52
5.36	Comparison between the four exposure times, CASES b.	54
5.37	Non-Aluminum Cases b, Maximum irradiance, $t_4=0.04$ s.	56
5.38	Aluminum Cases b, Maximum irradiance, $t_4=0.04$ s.	56
6.1	Simulations of UVC and blue LEDs with <i>TracePro</i>	58
6.2	Set-up for UVC and blue LED irradiation.	59
6.3	Steps of the experiments.	60
6.4	Post-exposure: experiments with 3 s and 5 s, 10 mL of contaminated water.	61
6.5	Post-exposure: experiments with 2 s, 20 mL of contaminated water.	62
6.6	Post-exposure: experiments with 2 s, 20 mL of contaminated water.	63
6.7	Simulated aluminum tube with <i>TracePro</i>	64
6.8	Irradiance simulation on a horizontal plane in the middle of the aluminum tube with <i>TracePro</i>	65
6.9	Irradiance simulation on a vertical plane in the middle of the aluminum tube with <i>TracePro</i>	66
6.10	Set-up for the Experimental Section 2.	67
6.11	Post-exposure: 1st set of tests on aluminum tube.	68
6.12	Post-exposure: 2nd set of tests on aluminum tube.	69
7.1	Set-up for blue-LED experiments.	75

7.2	Curcumin samples: 1) disk of white vinyl glue, 2) vinyl glue and curcumin disc with curcumin powder on the surface, 3) disk of mixed vinyl glue and curcumin, 4) thick pieces of vinyl glue and curcumin mixed, 5) disk of mixed resin and curcumin, 6) curcumin powder. . .	76
7.3	Tests 1-16.	77
7.4	Post irradiation vinyl glue disks residues.	78
7.5	Tests 1-7.	80
7.6	Reduction of different solutions of curcumin: powder curcumin and disk with glue and curcumin comparisons at different time exposure. . .	80

Acronyms

UV

Ultra-Violet

CW

Continuous Wave

PL

Pulsed Light

PS

Photosensitizer

LED

Light emitting diodes

UVGI

Germicidal ultraviolet radiation

LPUV

Low-pressure mercury lamps

PDT

Antimicrobial Photo-Dynamic Therapy

ROS

Reactive Oxygen Species

aBL

Antimicrobial Blue Light

GN

Gram-Negative

GP

Gram-Positive

PBL

Pulsed Blue Light

Chapter 1

Objectives, overview and structure of the thesis

This project aims at analyzing the efficacy of water sanitization through the use of Ultra-Violet (UVC) and blue radiation. The effectiveness of these light-based treatments have been tested by evaluating the evolution of *Enterobacteriaceae*, which find their natural habitat in human and other animals intestine, before and after the light application. Therefore, this work has pursued the followed objectives:

1. To demonstrate the effectiveness of the use of the germicidal UVC light.
2. To test the efficacy of the combined action of UVC and blue sources.
3. To provide a very simple solution to the 6th Sustainable Development Goal, about “Clean water and sanitation” by analyzing and testing a simple decontamination system based on a metallic pipe in which flows water to be sanitized.
4. To study the trade-offs that allow balancing the efficacy and costs of the LED sources for different configurations that have been analyzed through a MATLAB® program which, taking as input the number of LEDs and their respective desired positions along two parallel surfaces, returns the value of average and maximum irradiance at a given point in space.

The thesis is composed of nine chapters:

- *Chapter 1* describes the objectives and the structure of the thesis.
- *Chapter 2* provides the motivation from which this work starts, focusing, in particular, on radiation and its use in sterilization.
- *Chapter 3* describes the use of UVC for water disinfection studied in literature. It gives a description of the working principle of UVC radiation, with some examples of its application, it compares UVC-LEDs to the previous used low-pressure mercury lamps (LPUV), showing limits and advantages. It also provides a brief overview on Continuous Wave (CW) and Pulsed Light (PL) modes.
- *Chapter 4* covers the topic of the Photo-Dynamic Therapy and blue light, which are used as less harmful antimicrobial therapies than UVCs, explaining the working principles and their applications.
- *Chapter 5* is about the MATLAB® simulation of Lambertian sources arranged in different geometries, in order to find the best one that provides the correct radiant energy for a precise disinfection: it has been firstly implemented as a single UVC-LED, also validated with a commercial ray-tracing software, then there is the evaluation of the effect of adding more Lambertian sources on the same plane and finally on parallel planes. It also describes the implementation of a simple aluminum structure and the advantageous aspects of using it.
- *Chapter 6* shows the first experimental part, in which UVC and blue LED have been tested together to find a synergistic action of both in sanitizing contaminated solutions at different exposure times. Moreover, this chapter contains the experimental tests carried out on an aluminum tube demonstrator into which water to be disinfected flows, applying the previous simulations to a real hydraulic situation. Besides, in the final section, there is also a brief evaluation of the aluminum tube changing two different flow rates and diameters of the pipe itself.
- *Chapter 7* illustrates the second experimental part, in which a photosensitizer (curcumin) has been added to an aqueous solution to be sanitized with blue light. Different exposure times have been treated and the effect of various curcumin compositions have been evaluated.
- *Chapter 8* includes all the main reached results and contains the conclusions of this work.

Chapter 2

Introduction

The interest in light-based treatments in years is worldwide growing due to two main global problems: antibiotic resistance and the spread of COVID-19 pandemic outbreak.

Antibiotic resistance

Since the discovery of antibiotics, pathogens have been resistant to them: Fleming discovered penicillin in 1928; few years later, indeed, he exposed his studies on the presence of bacteria “easily resistant to penicillin”, making antibiotics ineffective. The development of pathogenic antibiotic resistance results from the overuse of antibiotics in the treatment of various diseases; it is valued that, for developing countries the annual consumption per person increases by a factor of 10 [1]. In addition, another contributing factor is the misuses of antibiotics in animal feed: an estimate has predicted that about 200,000 tons of antibiotics will be added in animal feed [1]; so it has become increasingly difficult to find solutions to eradicate the affecting bacteria. Over time, the problem of antibiotic resistance has been a major obstacle for health safety and, in order to overcome it, new non-antibiotic strategies for infections and disease have been experimented.

COVID-19 pandemic

In the last two years, the use of light for therapies has captured even more global attention due to the spread of the COVID19. Coronavirus disease 2019 (Covid-19) has been declared as a pandemic in March 2020 by the World Health Organization: it has been involving hundred of millions of people across the world, causing over 5 millions of deaths up to November 2021. COVID-19 is an infectious pathology causes by the virus SARS-CoV-2 that affects the respiratory system: in most cases it is cured without any particular treatment, while many other cases tend to develop

worse forms that require medical help, increasing hospitalizations and occupied places in intensive care. For these reasons, the Ultra-Violet radiation has been applied to prevent and limit its spread. More details will be provided in Chapter 3.1.2.

Lighth-based treatments

In this perspective are inserted the light-based therapies, antimicrobial therapies based on a non-antibiotic approach. Light-based therapies are recognized to be helpful in the limitation of these problems: their antimicrobial action against viruses, bacteria and fungi is applied to the study of disinfection systems for air, water and surfaces. This work is focused on the use of light-based therapies for water disinfection.

In 2015, the United Nations adopted the 17 Sustainable Development Goals (SDGs) to reach better human conditions, which can improve life on planet, by 2030 (Fig. 2.1). The 6th is about “Clean water and sanitation”: it aims at providing affordable and safe drinking water, investing in sanitation facilities, infrastructure and encouraging hygiene. Water disinfection is fundamental to ensure clean water and to prevent health issues that, over the years, have been strictly linked to waterborne epidemic infections.



Figure 2.1: Sustainable Development Goals in 2030.

Many of these infections are caused by a family of bacteria that affect the gastrointestinal system, the so called *Enterobacteriaceae*: their natural habitat is in the intestines of humans and other animals, acting as pathogens and causing dysentery, urinary tract infections and, in extreme cases, even deaths. One of the most recent examples is that of the bacterium *Citrobacter koseri*, which, in Ospedale Donna e Bambino di Borgo Trento, in Verona, from 2018 to 2020 involved 89 people, mainly new-borns admitted to intensive care, causing four deaths. After some analysis, it emerged that the bacterium would have been nested in water tap and on surfaces of some bottle feeding, due to a contamination to the water supply [2]. Therefore, it becomes necessary to rely on a safe water distribution system that provides adequate sanitation in accordance with sanitary needs to prevent the spread of infections and improve quality of life.

In this thesis work the action of UVC and Photo-Dynamic Therapy with blue LEDs have been analyzed to assess their germicidal effect against *Enterobacteriaceae* infections. Besides, various configurations of UVC-LED sources have been modeled: different geometries based on the calculation of the emitted irradiance have been evaluated in order to establish the correct number and arrangement of UVC-LEDs that better ensure an adequate antimicrobial efficacy, also in relation to optical powers of the LEDs and exposure times of irradiation.

2.1 Introduction to Radiation

The electromagnetic spectrum is the range of frequencies of radiation and their respective wavelengths and photon energies (Fig. 2.2). In general, the energy emitted from the electromagnetic radiation is calculated through the Planck's equation:

$$E = h\nu = \frac{hc}{\lambda} \quad (2.1)$$

where E is the photon energy (J), ν is the frequency (s^{-1}), λ is the wavelength (m), c the speed of light in vacuum ($3.0 \cdot 10^8 \text{m/s}$) and h is the Planck's constant ($6.62 \cdot 10^{-34} \text{J} \cdot \text{s}$).

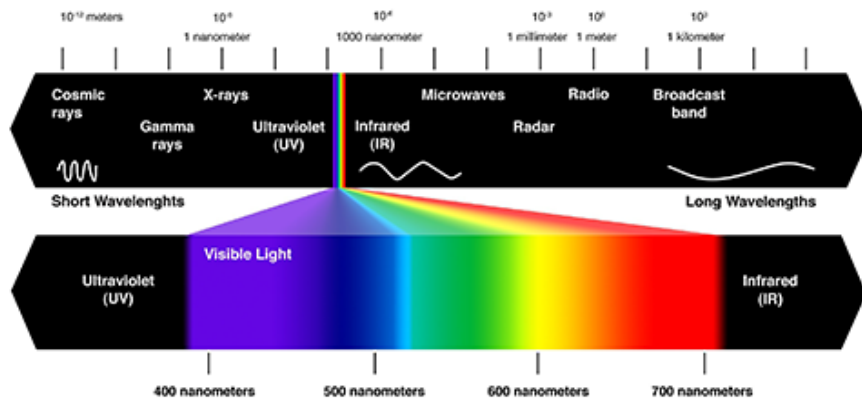


Figure 2.2: The electromagnetic spectrum [3].

It is important to distinguish radiation in:

- **Ionizing radiation:** characterized by high energies, up to 10-100 eV, are capable of modifying DNA and cell structures, transforming health cells into reactive and potential-dangerous cells; therefore it is important to carefully control them because, as the UV radiation on skin, their high energy is harmful and can induce diseases.

Ionizing radiations can be:

1. *Direct:* radiation of charged particles (electrons or protons, for example) that move into the matter of which is made of the target. Each particle provides its energy directly to matter through a series of Coulomb interactions; after every interaction, there is an exchange of energy between particles and atoms of the target with ionization of the atom itself as result.
2. *Indirect:* radiation of non-charged particles (gamma-photons or neutrons, for example) that transfer firstly the energy to charged particles; after the first ionization, they travel for a certain distance before ionizing other particles.

- **Non-ionizing radiation:** characterized by lower energy, under 10-100 eV, are unable to destabilize the atomic balance.

2.1.1 General parameters involved

The impact that ionizing radiation has on the matter can be studied and described considering the quantitative evaluation of the following parameters:

- *Radiant Power*: is the total radiant power emitted, (W);
- *Radiant Energy*: is the total radiant energy emitted on a time period, (J);
- *Irradiance*: is the total radiant power on an infinitesimal surface element with an area dS divided by the area, (mW/cm^2);
- *Fluence Rate*: is the total radiant power incident on a cross section dA of an infinitesimal sphere, over dA , (mW/cm^2);
- *Exposure Time*: is the time in which the irradiation is delivered, (s).
- *Dose*: is equal to the Fluence Rate (mW/cm^2) multiplied by the exposure time, (mJ/cm^2).

2.2 Mechanism of disinfection with Radiation

The action of disinfection through the use of radiation involves ionizing radiation in most cases. In general, when radiation interacts with living tissues, cellular deaths occur through two mechanisms (Fig. 2.3):

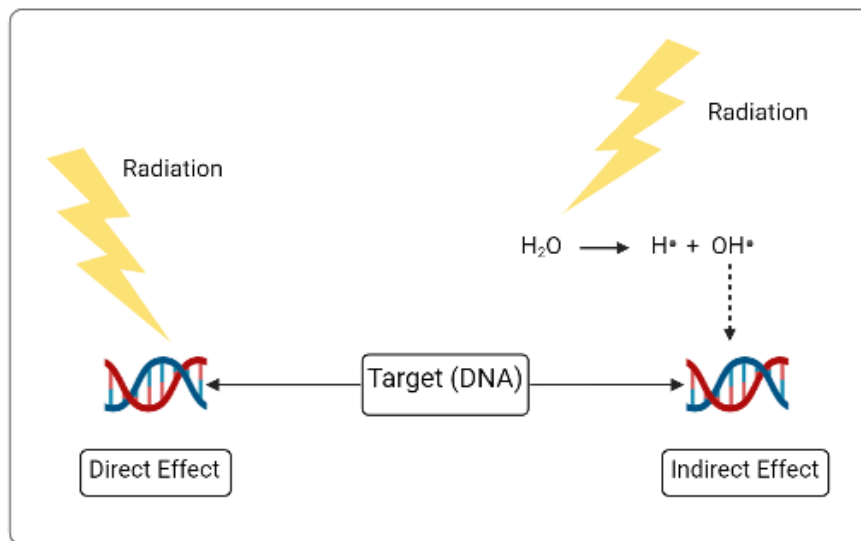


Figure 2.3: Mechanisms for cell damage by radiation: direct and indirect effect on DNA.

- **Direct mechanism:** the particles of radiation directly damage the cellular DNA. The two strands that make the DNA double helix carry the same

information and, when particles of ionizing radiation interact with them, the following three cases can occur (Fig. 2.4):

- *Case A*. Single-stranded break: a single particle ionises one of the two filaments: only one is broken and a repair mechanism can follow by the intact filament, forming a new one equal to itself.
- *Case B*. Double-stranded break 1: a single particle ionizes both DNA strands simultaneously, leading to cellular inability to repair damage and subsequent cell death.
- *Case C*. Double-stranded break 2: two different particles strike the two filaments separately at two different time instants: if the two times are very close, the repair mechanism cannot occur and ionization leads to the death of the affected cell.

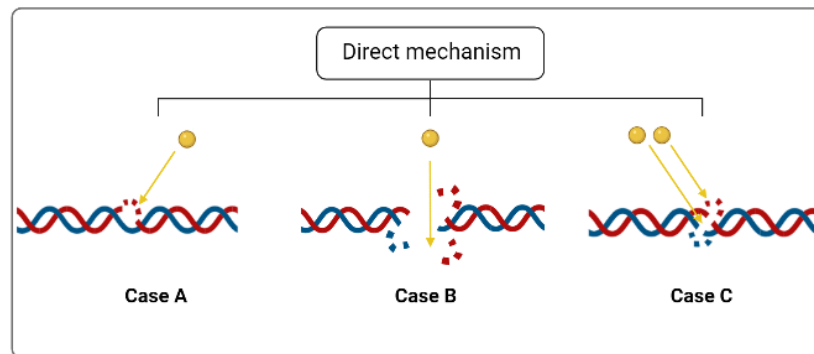


Figure 2.4: Direct mechanism for cell damage.

- **Indirect mechanism:** the particles of radiation do not interact directly with cellular DNA, but the surrounding molecules that interact with radiation are ionized and there is the production of free radicals, highly reactive and harmful for cellular life. The mechanism of the sanitification with radiation aims to “hit” water molecules: generally, when a photon invests these molecules, they can produce radicals, that can be considered as the products of “radiolysis”. These ROS (Reactive Oxygen Species) are small cytotoxic species that, in situ, are highly reactive and therefore able to chemical attack a large range of biomolecules, such as lipids, proteins, nucleic acids, destroying all the types of microbial cells, viruses and parasites. This action is clarified later.

This mechanism acts if the toxic products are high enough and transcription errors occur, which then result in microbial inactivation. Usually, each pathogen has a different sensitivity to radiation, requiring different irradiation

doses for the same inactivation fraction. The sensitivity level depends on several factors, in particular:

1. Size of pathogens and structural arrangement of DNA in the microbial cell: viruses are generally easier to kill because their small size, about 0.02 μm to 0.04 μm , whereas higher doses are required for bacterial damage, with a size of 0.2 μm to 0.4 μm .
2. Oxygen compound during the process that increases the lethal effect;
3. Water content: if a microorganism is in dry conditions it can develop higher resistance because of the lack of free radicals formed from water by radiation;
4. Temperature: over the range of 45 °C microbial cells react correctly to the ionizing process, whereas under the subfreezing temperature they can show resistance due to the behaviour of water cells at lower temperatures.

Therefore, for the disinfection process to be effective, it is necessary to take into account these parameters in order to achieve a more targeted treatment.

Chapter 3

Water Disinfection with UVC

*“Water, water, everywhere,
Nor any drop to drink!”
Samuel Taylor Coleridge*

Approximately one third of the world population is threatened by waterborne infections due to poor free access to clean water and limited sanitation. About 875 million people are affected each year by diarrhea, caused by contaminated water, which is responsible for 4.6 million deaths [4, 5]. Besides, it has been determined by the U.S. EPA that for a water supply to be drinkable and safe it must be 99.9% sanitized of pathogens [6], so the discovery of low cost and reliable technologies, is the goal many researchers want to achieve.

Since ancient times, people have been looking for solutions to get drinkable water: Aristotle advised the troops of Alessandro Magno to boil water before drinking it [7]. Heat, chlorine, ozone, filtration have been the main methodologies evaluated over time for bacterial removal from water. The use of some of these methods brought great disadvantages including high costs and constant energy; taste alteration occurs with chlorine, despite destroying bacterial nucleic acids by preventing gene transcription or high maintenance costs are required for filter systems. More recently, water disinfection methods that involved the use of natural substances have been discovered, such as ginger oil that achieves about 88% sterilization [5].

Moreover, it has always been popular the practice of sterilization by exposing containers filled with water to sunlight for several hours: the spectral component was found to belong to the band of near-ultraviolet (320 nm to 400 nm) and several studies have been carried out on the antimicrobial action of sunlight, UV at 254 nm [8]; however, this method has geographical and meteorological limitations [4].

So many researchers have tried more functional alternatives to the problem of

water sanitization and among them there are: Disinfection By-Products (DBPs), which use has been limited for a possible carcinogenic behaviours, ultrasounds, Ultrahigh Hydrostatic Pressure (UHP), nanomaterials, Ultra-violet and visible radiation [6]. Although the discovery of the antimicrobial action of UV radiation dates back to the late 1800s, the first applications for water sanitation date back to 1916, in the United States. Among the novel non-antibiotic strategies quoted above, Ultraviolet C therapy, Photo-dynamic therapy and blue-light treatments have been treated in this study.

In this chapter the action of Ultra-Violet (UVC) radiation is described.

3.1 Ultra-Violet C (UVC)

The electromagnetic spectrum range of 100 nm to 400 nm represents the UV irradiation. UV-light can be classified according to the following subdivisions (Fig. 3.1): Vacuum UV (100–200 nm), UVC (200–280 nm), UVB (280–315 nm) and UVA (315–400 nm).

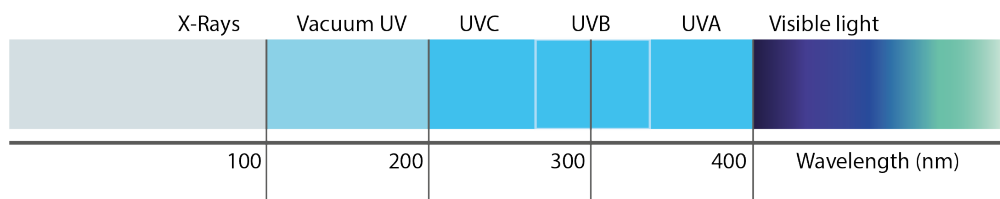


Figure 3.1: Ultraviolet radiation spectrum.

Ultraviolet radiation, and specifically UVC (200 nm to 280 nm), is widely known for its germicidal effect and it has also been demonstrated that its disinfectant power is far more relevant than the damage it can cause to host cells [9], so it has become of great interest. Over time, UVC light has been one of the most widely used methods for disinfecting water, air and surfaces, so much so that, in 2000, it was recognized by the U.S. Food and Drug Administration as an effective strategy for bacterial disinfection in food, beverage and water [10].

3.1.1 Operating principle

Germicidal ultraviolet radiation (UVGI) is commonly used to inactivate pathogenic microorganisms and UVC light is commonly assumed to have inhibitory properties capable of damaging their RNA or DNA: the absorption of a photon results in the formation of pyrimidine dimers between two thymine bases, 6-4 photo-products (Fig. 3.2). The bactericidal function is achieved because this mechanism creates

errors in translation and transcription mechanisms of these sequences, which then lead to the complete inhibition of microbial replication and their subsequent death.

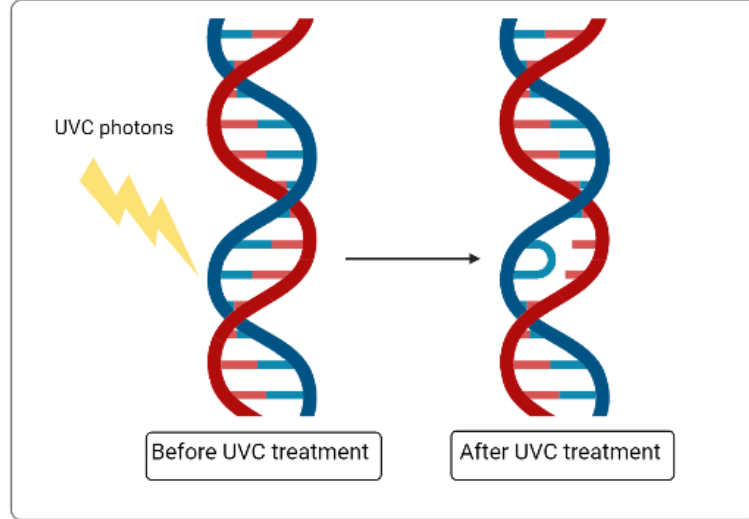


Figure 3.2: UVC inactivation mechanism.

The general equation for microbial inactivation is:

$$\text{Log reduction} = \log \frac{N_d}{N_0} \quad (3.1)$$

where N_d is the concentration of bacteria after the light treatment (CFU/mL) and N_0 is the initial concentration of non-irradiated bacterium (CFU/mL). This formula allows evaluating the reduction in bacterial concentration after the UVC radiation exposure.

As mentioned in *Section 2.2*, when radiation do not damage entirely both strands, after the UV-treatment, two mechanisms of DNA repair can occur:

- *photoreactivation*, by attachment to the dimers of the photolyase enzyme, which is light-dependent and requires wavelengths of 300–500 nm; it increases with the rising of visible light intensity and temperature, while high UV fluence tend to decrease this mechanism.
- *repair by excision of nucleotides (dark repair)*, which is instead independent from light, in which the synthesized segment replaces the broken one [6]. This is the case of the single-stranded break, represented in the Case A of Figure 2.4.

A quantitative assessment of the photo-reactivation processes is provided by the following equation:

$$\text{Percentage of photo - reactivation (\%)} = \frac{(N_t - N)}{(N_0 - N)} \times 100 \% \quad (3.2)$$

where N_0 are the initial cells, N_t (CFU/mL) is the number of cells after the photo-reactivation for a time period t (h) and the degree of photo-reactivation indicates the fraction of photo-reactivated cells from inactivated ones [11].

As it can be imagined, DNA repair mechanisms do not cooperate in achieving efficient bacterial inactivation and increase the likelihood of new infections occurring; due to this, a targeted disinfection irradiation is needed for antibacterial aims, to not allow pathogens to develop reactivation following treatments.

3.1.2 UVC-light for COVID-19

Several studies have been conducted to try to limit contagions of the disease through UVC-radiation for air and surface decontamination. It has been verified that COVID-19 can remain in aerosols for about 3 hours, so various room disinfection systems have been discovered. Considering the carcinogenic potential of UV, far-UVC light (222 nm) are used in one of the studies, within limits exposure limit (3 mJ/cm²/h): it has demonstrated the efficacy they had already shown for other coronaviruses, similar in genomic size, resulting in 90% of inactivation after 8 min of treatment with 0.39 mJ/cm² and in 99.9% with 1.2 mJ/cm², for 25 minutes [12].

Moreover, it has been considered the idea to irradiate surfaces and N95 respirators to reuse them and limit the environmental impact, exploiting the UVC properties: the Centers for Disease Control and Prevention (CDC) recognised a UVC dose of 1 J/cm² with the assurance of not finding any residual virus on any surfaces [13].

3.2 Introduction to Light Emitting Diodes

Light emitting diodes (LEDs) are widely used for many electronic applications that are commonly used in everyday life. LED are composed of a thin layer of a semiconductor material: initially it is a conductor, with no free electrons and with high cohesion between atoms; then it undergoes a doping process through the addition of atoms of different elements, in which impurities are formed, altering the material stability and creating holes and free electrons.

The discovery of LED technology dates back to the 1960s when a group of scientists created a positive-negative junction (p-n) experimenting a chip composed of a semiconductor material [14].

A p-n junction is formed by joining two sections:

1. *N-Type*: negative, so called because there is an increased amount of *electrons*.
2. *P-Type*: positive, so called because there is an abundance of formed *holes*.

The direction of the current goes from the P-Type region to the N-Type region, not in the contrary. In order to allow the electronic transition, it is necessary to connect the negative electrode (cathode) of a circuit to the N-Type material and the positive electrode (anode) to the P-Type material: in this way, the electrons in the N-Type section are attracted by the positive electrode (anode) and otherwise with the holes in the P-Type material. Three situations can occur:

- No applied voltage: if no voltage is applied, a *depletion zone* is formed along the junction of the two layers. It is a non-conductive zone where the electrons of the N-type material fill the holes of the P-type material, the *recombination process*, preventing the passage of electrical energy, as they cancel each other charge out.
- Forward-Bias applied: the negative section is connected to the cathode, whereas to the positive terminal is connected the anode (Fig. 3.3). In the forward bias the depletion zone is narrowed because of the rejection of holes from the P-Type region and of the free electrons from the N-type region. Then electrons and holes are pushed towards the p-n junction, minimizing the depletion zone so that it becomes thinner and more conductive. Electrons, in this way, are able to access the P-Type region, allowing current to flow from the negative to the positive electrode of the battery. LEDs convert electrical energy into light energy when forward polarized.
- Reverse-Bias Applied: there is a reversal of polarization (Fig. 3.4). The result is a removal of holes and electrons from the p-n junction and a consequent increase of the non-conductive depletion zone. If the depletion barrier expands, it is also difficult to let electrons move into the diode, increasing the electric resistance of the material.

Light Emission

It is known from Quantum Physics that electrons are located in atomic orbitals and possess different energies based on the energy levels they occupy. The result of their transitions within different energy layers is the absorption or emission of a quantum of energy, photon, depending on whether they go from a lower to a higher energy state or vice-versa. In particular, the energy of the emitted photons depends on the energy gap between the conduction and the valence band,

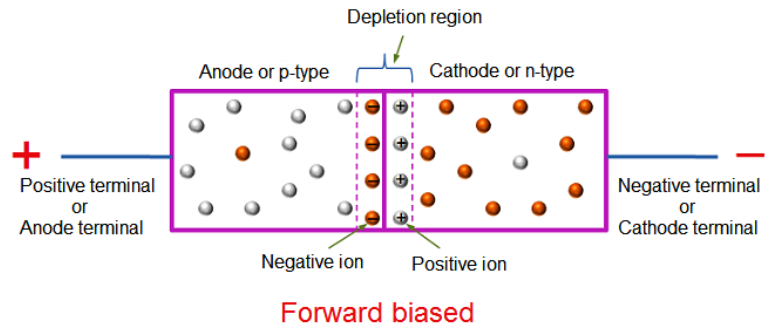


Figure 3.3: Forward-bias for p-n semiconductor junction [15].

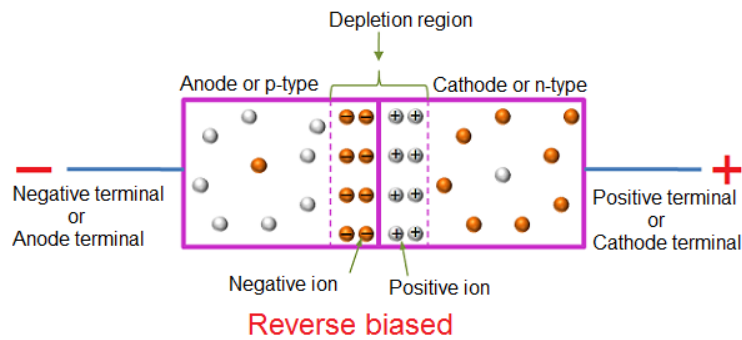


Figure 3.4: Reverse-bias for p-n semiconductor junction [15].

which therefore determines the color of the emitted light. Emission in the visible spectrum requires a larger energy gap than, for example, emission in the infrared. Therefore, changing the compositions of semiconductor alloys that constitute the LED structure, allows selecting different emission wavelengths. For the shorter range of the visible spectrum, Gallium Indium Nitride (GaInN) is used for near ultraviolet, green and blue LEDs and Aluminium Gallium Nitride (AlGaIn) for ultraviolet LEDs [14].

Structure

The p-n junction is generally placed in a bulb of transparent epoxy hard plastic for the junction protection and to allow better direction of the light. Since the light output of a LED is not high, the bulb allows the reflection of light photons that are emitted from the junction towards the rounded top, which acts as a converging lens, concentrating all the light. However, the general epoxy structure of LEDs can vary, taking cylindrical or rectangular shapes.

3.3 UVC-Light emitting diodes

This section discusses the characteristics and applications of UVC LEDs, in comparison with previously used low-pressure mercury lamps, and lists some examples of studies in the literature.

3.3.1 Low pressure ultraviolet (LPUV)

Low-pressure mercury lamps (LPUV) have been largely used to generate UV radiation for UVGI applications. They are characterized by an almost purely monochromatic emission at about 254 nm and a favorable cost per emitted watt ratio. On the down side, they have long warm-up times that result in the impossibility to rapidly switch on and off, have a bulky structure, and pretty short bulb lifetime (4-1000 hours). However, their main limitation is their intrinsic working principle that requires mercury and in the Minamata Convention (2013), the United Nations Environment Programme (UNEP) imposed limits on the use of the amount of mercury [16] because of its toxic properties that can contaminate the environment.

3.3.2 UVC-LEDs

The ultraviolet light-emitting diode (UVC-LEDs) has become a valid technology to substitute mercury lamps in germicidal applications. UVC-LEDs are p-n junction semiconductors employed for water, air and surfaces disinfection against bacteria, but also with anti-viral and anti-fungal efficiency. Among the several advantages of LEDs, there are: compact and small size (5-9 mm in diameter) that simplifies the integration in sterilization devices; no-warm up time required, so it is possible to turn-on and off instantaneously regardless the variation of the external temperature [16]; low voltage operation that enables their use also with batteries and solar cells, so that they can be used in areas where there is no continuous power supply [17]. Moreover, they have low maintenance and longer replacement intervals (up to 100,000 h [18]). Finally, unlike LPUVs, for UVC-LEDs it is possible to utilize optical lenses and reflectors to have a different radiation profile, mainly balloon-shaped (Fig. 3.5) or heart-shaped [17].

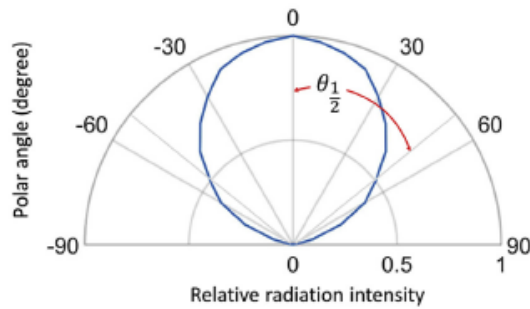


Figure 3.5: Balloon-shaped irradiation profile [17].

The most important feature lies in the variability of the emitted radiation: in fact, contrary to mercury lamps, UVC-LEDs emit radiations of different wavelengths (in a range of 245–370 nm). This is a fundamental feature for microbial inactivation devices because, in general, the disinfection capacity increases when the provided wavelength peak is close to the maximum absorption of the spectrum of the pathogenic DNA, generally around 165 nm, and having a wide range of possibilities for several microorganisms makes UVC-LEDs a strong antimicrobial device (Fig. 3.6).

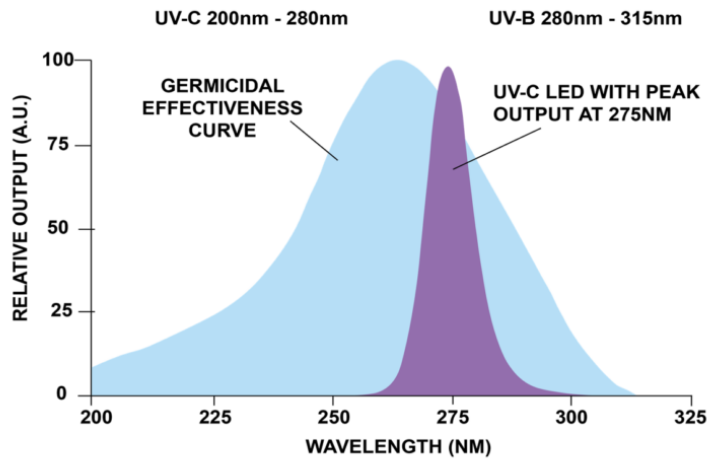


Figure 3.6: UVC-LED peak at 275 nm and germicidal effectiveness curve [19].

3.3.3 Comparison between UVC-LEDs and LPUV

The main differences between UVC-LEDs and LPUV lamps are summarized in Tab.3.1: the toxic content of LPUV, missing in UV-LEDs, the bulky structure of LP mercury lamps compared with the small size of LEDs, long warm-up times to reach stable conditions for 254 nm (LP), the narrow spike of irradiance, corresponding to the monochromatic radiation of LPUV versus the polychromatic spectrum, with variable irradiances of UV-LEDs (Fig. 3.7), and the lower output power of UV-LEDs, tens of milliwatts, against the higher of LPUVs on the order of watts.

Several studies have compared both technologies: in one of them on the inactivation mechanism between UV-LEDs and LPUV on fungal spores (*Aspergillus niger*, *Penicillium polonicum*, *Trichoderma harzianum*), emerged that the warm-up times for the former was of 5 min against the 30 min required for the latter; the inactivation rate constant (k) in 254 nm (LP) were lower ($k_{254} = 0.04\text{-}0.09 \text{ cm}^2/\text{mJ}$) than that of UV-LEDs ($k_{265} = 0.07 - 0.11 \text{ cm}^2/\text{mJ}$) and that it was relevant the resulting superiority of UVC-LEDs over LPUVs in controlling fungal photoreaction, despite their higher energy consumption [20], about 25-40 times greater [21].

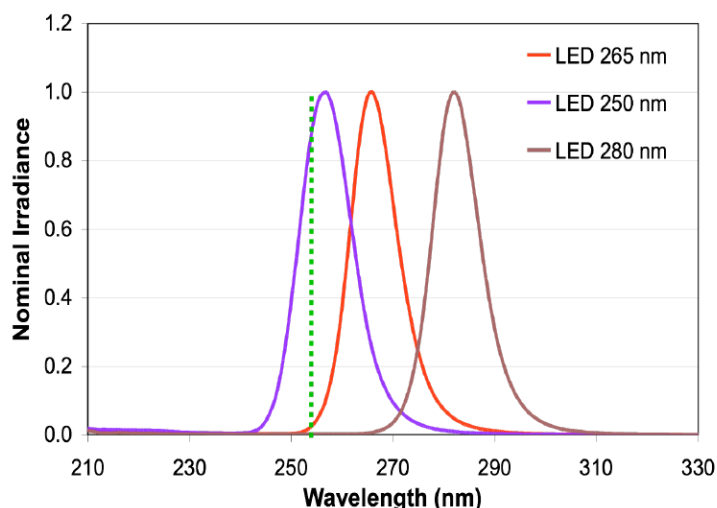


Figure 3.7: Nominal irradiance of three LEDs compared to the narrow spike of LP lamps (in green, 254 nm), [22].

The antimicrobial action for 254 nm and UV-LEDs 265 nm were examined in following studies on bacteria (*Escherichia Coli*, *Pseudomonas aeruginosa*, *Legionella pneumophila*) and viruses (*Bacteriophage QB*): in general, pathogenic inactivation with 265 nm UV-LEDs showed the best results and the reason is linked to the peak of absorbance of nucleic acid, close to 260 nm [21], (Fig. 3.6). Therefore, long exposure times are required for UVC-LEDs to have the same significant microbial

disinfection as mercury lamps [23].

Table 3.1: LPUV lamps vs UVC-LEDs.

	LPUV lamps	UV-LEDs
Wavelength	254 nm	Polychromatic
Warm-un time	Long (minutes)	Short (seconds)
Structure	Bulky	Small
Mercury	Yes	No
Temperature dependence	Yes	No
Exposure time	Short	Long
Electrical consumption	Low	High
Output power	High (W)	Low (mW)
Inactivation efficiency	High (40%)	Low (5-15%)
Lifetime	>10.000 h	>100,000 h

3.3.4 UVC-LEDs Limits

From studies on the application of UVC radiation on surfaces and liquids, it has emerged that their use is limited to superficial disinfection because of the limited penetration of short wavelength light. Besides, due to the high energy of the Ultraviolet light, UV exposure times of host cells were evaluated and it was found that prolonged exposures on human cells may produce carcinogenic and potentially harmful effects on non-target cells. Fortunately, it has also been shown that DNA repair enzymes are able to repair the damage quite quickly [24]. Moreover, as mentioned above, the other disadvantage in the use of LED is the low power emitted, so a careful evaluation to improve the penetration depth and the efficacy of the irradiation, finding different solutions with LEDs arranged in different configurations is necessary: this thesis works on this purpose. Several UV-LEDs geometries have been studied in order to propose a valid solutions to the low UV-LEDs output power.

3.3.5 State of the art

The effects of UVC treatment using LEDs have been extensively studied over time, and several factors that can affect the effectiveness of the treatment have been identified: cell structure, cell thickness and integrity of the wall, susceptibility to photoproducts generated as a result of irradiation, the state of the microorganism and the ability of the cell to set up repair mechanisms. Several studies have been carried on the effect of UV-LEDs on different microbial species: Gram Positive, Gram Negative bacteria, Viruses and Yeasts.

Bacterial cells are divided into two main groups: Gram Positive and Gram Negative. The differences between the two types are in their external cell wall structure: the exterior membranes of Gram Negative bacteria have an organised and compact structure, so they prevent the diffusion of undesired molecules inside the cell, behaving as a porous filter; whereas in Gram Positive bacteria the outer wall (tens of nm thick) porosity is higher, facilitating the entry of various substances.

Studies reported many positive experimental results on application of UVC-LEDs about the inactivation of bacteria *Staphylococcus aureus* (MRSA), *Enterococcus faecalis* (VRE), *Staphylococcus*, *Streptococcus*, *E.coli*, *P.aeruginosa* and fungi like *Aspergillus fumigatus* and *Candida albicans*. The need of higher dose utilization to destroy fungal cells is emerged, maybe due to their different wall structure, with glycoproteins and glucans, that act as obstacles [24].

A study described the bactericidal result of 266 nm and 279 nm UVC-LEDs, comparing the effect of the same delivered dose to Gram-Positive (*L. monocytogenes* and *S.aureus*), with about 4-log reduction for 0.2 mJ/cm² and 5-log reduction for 0.6 mJ/cm², to Gram-Negative (*E.coli* and *Salmonella*) with respectively about 1-log reduction with the lowest dose and 3-5 log reduction for the highest and to yeasts, with about a final 1-log reduction for *P.membranaefaciens* and *S.pastorianus*. The resulting efficacy sequence is GN > GP > Y and the comparison between the two wavelengths underlined the best action of the 266 nm UVC-LED for its major ability of damaging DNA due to the production of ROS [25].

The wavelength-dependent sensitivity of *E. coli* and the effect of incident irradiance were also proven in another study, in 2021, that compared UVC-LED of 265 nm, 276 nm, 285 nm and 295 nm and showed that for lower wavelengths, i.e. 265 nm, the ROS damage is more significant than for the others, as it is in correspondence of the peak of DNA absorption and they assessed that the inactivation did not depend on the incident irradiance, whereas irradiance and exposure times were relevant for the higher wavelengths, to which low irradiances and long exposure times showed better results [26].

For viruses, however, the loss of viral infectivity is associated to an UV-induced damage to viral proteins: a study on *Adenovirus*, a waterborne virus particularly resistant to UV radiations, described the 66-89% and 80-93% of reduction of the initial amount of protein reached with respectively with 261 nm and 278 nm with a dose of 400 mJ/cm² [27].

3.4 Continuous Wave (CW) and Pulsed light (PL) modes

The disinfection using UV light can be delivered in two modes: continuous wave (CW) and pulsed light (PL) modes. The former irradiation is commonly used with

low light intensities while the latter provides short pulses of high intensity. Both are possible if UVC-LEDs are used, because of the capability of quickly turning-on and -off, but understanding the differences between the two modes and their behaviour with pathogenic microorganisms is not easy at all.

Actually, the few available studies show widely divergent results between the two modalities in microbial inactivation: about 2-log reductions with CW UVC-LEDs and 3-log reductions of *E. coli* with the pulsed treatment have been shown, but with no substantial differences. Better results, on the other hand, are obtained by comparing different frequencies and duty ratios: higher duty-ratio corresponds to better results in terms of bacterial decrease [28], [11].

Moreover, the increasing temperature after the light-treatment has been little analyzed and the few results exposed a considerable temperature increment in treatments with CW (29 °C to 42 °C, in 60 s) [11].

Chapter 4

Water Disinfection with PDT and Blue light

4.1 Photodynamic Therapy (PDT)

Antimicrobial Photo-Dynamic therapy (aPDT) is the other important subject in light-based therapies. It is based on three main factors: a pre-applied non-toxic photoreactive dye or photosensitizer (PS), that absorbs low-power visible light at specific wavelength and transfers it to oxygen, producing cytotoxic and harmful radicals.

The idea came from the Greeks, Indians and Egyptians, who started developing the functionality of light as therapy, although it was necessary to wait for the 20th century for further clarifications. Niels Finsen, a Danish physicist, tested the application of heat and light to cure the so called *Lupus Vulgaris* [29], a cutaneous tubercles, but the mechanism was described in Munich, 1900, observing the efficacy of inactivation of the pigment acridine orange coupled with light on *Paramecia*, by Raab. Later Von Tappeiner and Jodbauer, coined the term “photodynamic” observing the need of oxygen for the resulting mechanism, and in 1976 Weishaupt Gomer and Dougherty described the photochemical PDT operation by observing the removal of cancer cells with hematoporphyrin and exposed to red light because of the presence of singlet molecular oxygen [1].

The initial application of PDT was accepted as pre-cancerous treatment for skin lesions by the Food and Drug Administration [29], only after 1990s it has been used for antimicrobial purposing. The difference in the use of PDT between anticancer and antimicrobial therapy is that for the first the photosensitizer is delivered in the blood system with light-time intervals of many hours, whereas the application is on the surface of the infection with limited time (minutes) for the second.

4.1.1 Operating principle

As already mentioned, the PDT working principle uses oxygen molecules excited by visible-light with wavelength compatible with the absorption spectrum of the used PS.

The mechanism is represented in Fig. 4.1: there is the initial absorption of a photon from the PS in its ground-state that allows its conversion from singlet to triplet state. The excited PS can react with the surrounding oxygen molecules and undergo electron transfer (Type 1) to create superoxide and hydrogen peroxide (HO^* and H_2O_2) or have energy transfer (Type 2) forming reactive singlet oxygen ($^1\text{O}_2$) through the interaction with triplet ground state oxygen ($^3\text{O}_2$).

These Reactive Oxygen Species (HO^* and $^1\text{O}_2$) are highly reactive and therefore able to chemically attack, where they are produced and in accurate positions, a large range of biomolecules, such as lipids, proteins, nucleic acids, destroying all the types of microbial cells, viruses and parasites [1].

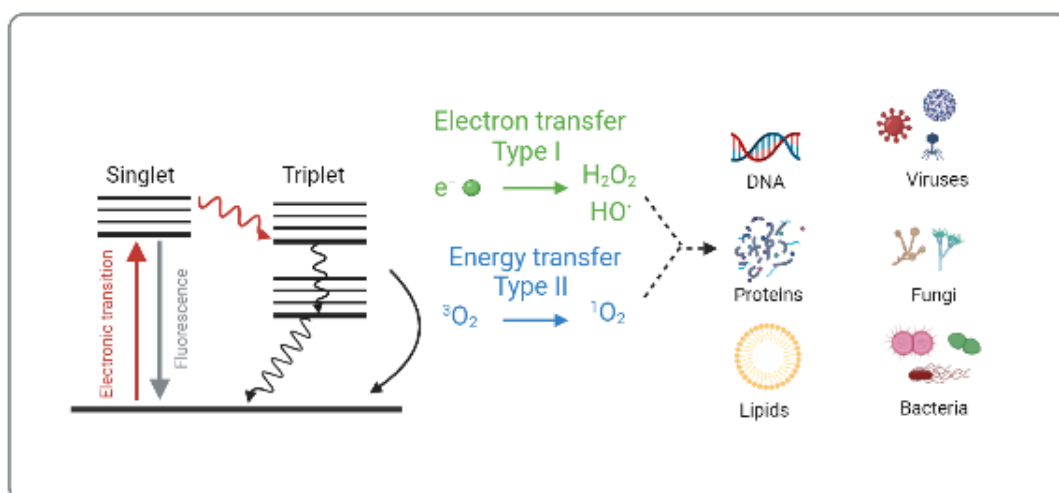


Figure 4.1: PDT working mechanism.

4.1.2 Photosensitizers

The choice of an optimal photosensitizer for the photodynamic therapy is based on the following requests: it must be non-toxic and show toxicity only after the light-treatment, it might be very selective for microbial and host cells and able to produce high ROS quantities. The selectivity for cells is evaluated in studies and it emerged that bacteria are more sensitive to PDT than host cells maybe because of the barrier function of nuclear membrane in mammalian cells; besides,

also differences in structure and dimension suggested that it is easier to kill bacteria for their 25-50 times smaller size than mammalian cells [9].

Some natural molecules are employed as PS, like porphyrins, that absorb in the range 400 nm to 700 nm. The inactivation mechanism of PDT varies according to the outer membrane structure of the targeted pathogen: for instance, the sensitivity to PDT of Gram-Positive is higher respect to Gram-Negative bacteria, due to their superior porosity that let PS enter the cell and activate the treatment. For this reason, cationic charges are used to overcome Gram-Negative resistance: with “self-promoted uptake”, Mg^{+2} and Ca^{+2} are exposed on the outer membrane and the membrane breakage is verified because there is the PS absorption of light, due to the permeability of the membrane itself, so Gram-Negative bacteria become PDT sensitive, too [1].

In literature, various PSs that be excited with visible light are reported; for example, Rose Bengal, TiO_2 , methylene-blue, curcumin, toluidine-blue and Chlorin(e6) [29].

4.2 Blue-light

The use of blue-light in the range of 400 nm to 470 nm is collocated between the non-antibiotic treatments to inactivate pathogenic microorganisms. Darwin, in 1886, was the first to report a phototropic response due to blue-light and it has become so relevant in the disinfection-field because, differently from ultraviolet irradiation, its behaviour is not so harmful for host cells. The antimicrobial blue-light is attracting attention because it exploit non-exogenous agents, as those required for PDT.

4.2.1 Operating Principle

Blue light has showed intrinsic properties because of it uses endogenous photosensitizing dyes to cause cell deaths. Despite the right antimicrobial mechanism is not so clear yet, the leading thesis is that after the photon absorption by endogenous porphyrins or flavins, the production of ROS occurs. It is an advantageous method because porphyrins are naturally produced by bacteria and microorganisms, so no extra-agents are required. Cell membrane damage, DNA oxidation and other modifications indicate the aBL correct operation but to different photo-inactivation kinetics correspond different types and sub-types of porphyrin: every bacteria is able to produce its own porphyrin, different from the other, so a different wavelengths is needed for each pathogen stimulation.

4.2.2 State of the art

Recent studies show that 405 nm blue-LEDs, used in the range of 7.5 - 270.0 J/cm², has a great germicidal activity on ESKAPE bacteria (*Enterococcus*, *Staphylococcus Aureus*, *Klebsiella Pneumoniae*, *Acinetobacter Baumtnnii*, *Pseudomonas Aeruginosa*, *Enterobacter*), with their resistances that “eskape” from antibiotic therapy [30].

In many of the experiments on the lethal action of blue-light, Gram-Positive bacteria were more responsive than Gram-Negative bacteria [1]. Between Gram-negative bacteria, it was studied the inactivation of *Legionella Rubrilucens* and great doses of 300 J/cm² and 500 J/cm² were necessary with 450 nm and 470 nm aBL, respectively, to have a 5-log-reduction [31]; with 470 nm and a dose of 234 J/cm² (60 mW/cm² and 60 min) is possible to obtain a 3.70-log-reduction of the bacterium *Neisseria Gonorrhoeae* [gonorrhoeae]. Among Gram-Positive bacteria, for methicillin-resistant *Staphylococcus aureus* (MRSA) lower doses than GN (55 mJ/cm²) of aBL are sufficient to suppress the totality of the culture using wavelengths of 405 and 470 nm [32]; the antimicrobial action is also demonstrated with pyocyanin to better manage the therapeutical treatment of MRSA infection [33].

Moreover, studies on aBL described the clinical possible application of blue-light against *P.acnes* lesions and digestive troubles from *H. pylori* [24]; it is also employed in dentistry, in combination with different dyes against the Gram-Positive *Streptococcus mutans*, *L. acidophilus*, which is responsible for caries: in particular the use of curcumin with blue-diode laser (405 nm) revealed a reduction of 78.92% with a fluence of 10 J/cm² and of 99.26% with 30 J/cm², proving the effectiveness of the yellow plant, even if its not clear its mechanism [34]. In this thesis work curcumin has been chosen as natural photosensitizer to better analyze its interaction with blue-light for water disinfection.

The main limitation of PDT therapy is the reduced penetration of blue light in living tissues, approximately <1mm for aBL.

4.3 Continuous Wave (CW) and Pulsed Light (PL) modes

The novel pulsed blue light (PBL) treatment is based on sequences of pulses interspersed with off-times that can excite molecules as porphyrins with specific times and irradiances and that can lead them to return in their non-excited state. The ability of allowing the PSs to randomly return to the ground state rather than simultaneously, as in CW, makes this technology more effective than CW, but less harmful than UVs [35].

PBL application has been evaluated and considered by various studies both on bacteria and viruses: one of them showed the superiority of PBL over continuous mode, testing two duty cycles (20% and 33%) at 450 nm *Propionibacterium acnes*: results reported that bacteria revealed a better success with the highest rate and that time of repetition of the treatment has a great relevance. This happened because the administration of different pulsed irradiances at specific time intervals allowed a total bacteria reduction due to the synchronization with their reactivation cycles [36]. Besides, evidences on PBL inactivation towards *Methicillin Resistant Staphylococcus Aureus (MRSA)*, showed that about 40-100 times less delivery of irradiance is required than that in continuous blue-light mode [35].

In other experiments, it was found that blue-light affects both the virus particle and envelope, altering the structure and inactivating it without the use of endogenous/exogenous PS, only by compromising the reverse transcription process. In the same study, it also emerged that PBL with 405 nm has a powerful incidence on beta-coronavirus, with an enhanced effect at high irradiances (12 mW/cm^2) with a dose of 130 J/cm^2 [37].

Chapter 5

Simulation of LED-based sources

This chapter is intended to provide an analytical discussion on the functioning of LEDs and to describe a simple quantitative characterization of the behaviour and the spatial distribution of the emitted irradiance by the LED source, previously theoretical described in *Section 3.2*.

5.1 LED simulation

Radiometry is the study of the energetic content of a radiation and the observation of its propagation behaviour in passing from a source to a detector. In this study, law of geometric optic are employed, diffraction and interference are neglected and a medium without any losses is considered. The mathematical general quantities are introduced:

1. **Radiant power** (ϕ_e) is the total radiant power emitted, where Q_e is the Radiant energy, [W]:

$$\Phi_e = \frac{dQ_e}{dt} \quad (5.1)$$

2. **Irradiance, or flux density** (E), is the total radiant power on an infinitesimal surface per unit area, [W/m²]:

$$E = \frac{d\Phi_e}{\cos \theta_d dA_d} \quad (5.2)$$

where the normal of the infinitesimal element of a surface (dA_d), forms the angle θ_d with the direction of the radiation; “d” stands for detector.

3. **Radiant Intensity** (I_e) is the radiant power of a source in a certain direction of emission, [W/sr]:

$$I_e = I_{e,\Omega} = \frac{d\phi_e}{d\Omega} \quad (5.3)$$

4. **Radiance** (L) is the radiant power over an infinitesimal element of solid angle and projected area, forming an angle θ_s with the normal of the surface element, [W/sr m²]:

$$L = \frac{\partial^2 \Phi_e}{\cos \theta_s \partial A_s \partial \Omega} \quad (5.4)$$

where “s” stands for source.

The LED treated in this work is a LED without lens, so it is modeled as an ideal Lambertian source.

5.1.1 Lambertian source

A Lambertian source is a source that emits homogeneously in all directions with an uniform radiance on the irradiated surface. The LED is considered as a circular source (Fig. 5.1), with diameter w , at a distance h from the surface containing the irradiated point X , with a given radiant power Φ_e and with the angle between the normal to the surface and the 3 dB ray $\theta_{3dB} = 60^\circ$. As the source, of area A , radiates over the entire hemisphere, radiance is considered constant:

$$L = \frac{\phi_e}{\pi A} = \text{const} \quad (5.5)$$

The irradiance that lies on the axis of the source, i.e. normal through the center of the source, is

$$E = L \sin^2 \theta_{\max} = \frac{\phi_e}{\pi A} \sin^2 \theta_{\max} \quad (5.6)$$

with

$$\theta_{\max} = \arctan\left(\frac{w}{2h}\right); \quad A = \pi \frac{w^2}{4} \quad (5.7)$$

Remembering the relation:

$$\sin(\arctan(x)) = \frac{x}{\sqrt{1+x^2}} \quad (5.8)$$

the maximum irradiance value is written as

$$E = \frac{4\Phi_e}{\pi(4h^2 + w^2)} \quad (5.9)$$

Instead, if the considered point is not on the source axis, the correction factor “*cosine fourth*” is supplemented in the equation, in which ϕ is the angle that the line source-point forms with the normal. The following is the formula of the irradiance of the point that has been implemented in MATLAB®, [38]:

$$E(\phi) = E(0) \cos^4 \phi = \frac{4\Phi_e}{\pi(4h^2 + w^2)} \cos^4 \arctan\left(\frac{r}{h}\right) = \frac{4\Phi_e}{\pi(4h^2 + w^2)} \frac{h^4}{(h^2 + r^2)^2} \quad (5.10)$$

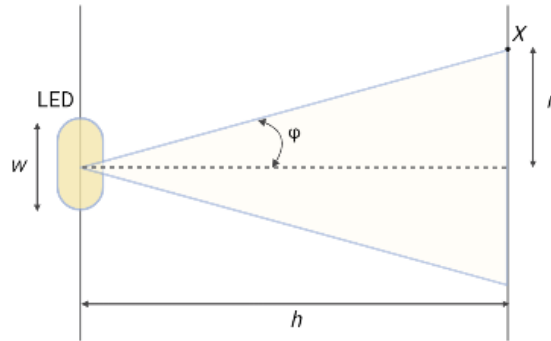


Figure 5.1: Circular source of diameter w , irradiating a plane in which the point X dists h from the source and r from its normal, forming an angle ϕ .

5.2 Single source on a plane

The simulated LED source has been considered to be circular with diameter $w = 8$ mm. The first step of this work concerns the representation on MATLAB® of the LED as Lambertian source.

5.2.1 CASE 1a

1 LED

The equation 5.10 has been implemented to evaluate the irradiance of a single LED placed at the center of a plane of 4×4 cm. The designed LED has the following features:

- diameter: $w = 8$ mm,
- radiant power: $\Phi_e = 100$ mW,
- coordinates: $P = (0,0)$,
- distance of the irradiated surface: $h = 1$ cm.

The resulting contour plot and pseudo-color plot of irradiance on the selected surface are displayed in Fig. 5.2 and 5.3. The maximum of irradiance, E , in the inner red circumference, corresponds to the center of the LED source, reaching a peak value of 27 mW/cm², whereas lowest values are along the outer circumferences.

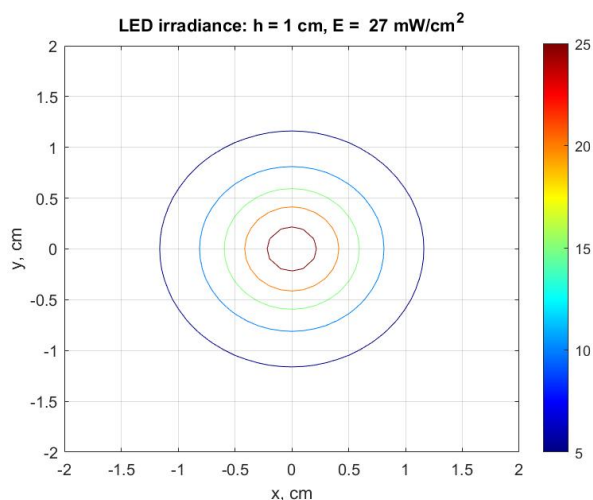


Figure 5.2: Contour plot of the irradiance of the LED at a distance of $h = 1$ cm from the surface, CASE 1a.

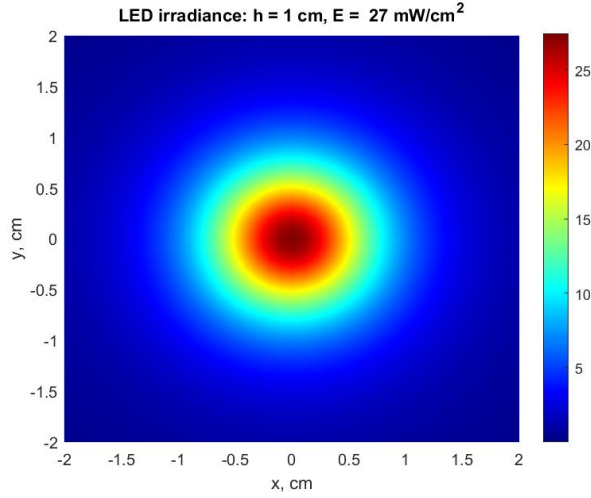


Figure 5.3: Contour plot and Pseudo-color plot of irradiance of the LED at a distance of $h = 1 \text{ cm}$ from the surface, CASE 1a.

Table 5.1: Maximum of irradiance at different distances h , Case 1a.

Maximum of irradiance (mW/cm^2)	h_1	h_2	h_3	h_4	h_5	h_6	h_7	h_8
Case 1a	137	77	44	27	18	13	10	8

Then, LED radiation at different distances has been evaluated to assess the light diffusion from the source to the surrounding space (Fig. 5.4). This is a fundamental step as selecting the correct distances is necessary for experiments in order to deliver the right fluence to the target and to assure a correct efficacy of disinfection.

The evaluation has been performed by observing parallel incidence surfaces h placed at varying distances from the source, spaced of 0.25 cm apart: the initial off-set viewing distance has been set to 0.25 cm because it has been seen that, at very small distances, the LED radiation has uninformative values and behaviour, with a non-linear peak of irradiance; instead, the final distance is at 2 cm , thus making a total of eight measurements. The following plots have been obtained:

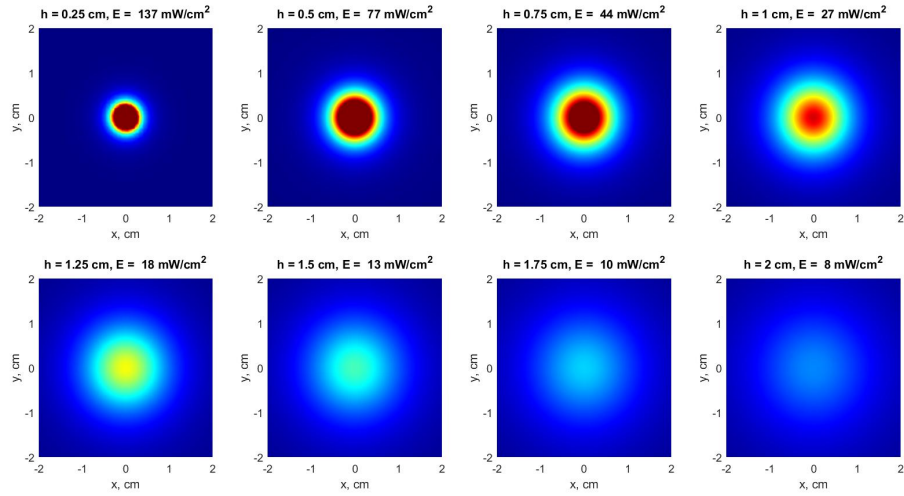


Figure 5.4: Pseudo-color plot of the variation of LED intensity: different distances (h) of the surface and the corresponding maximum of irradiance (E), CASE 1a.

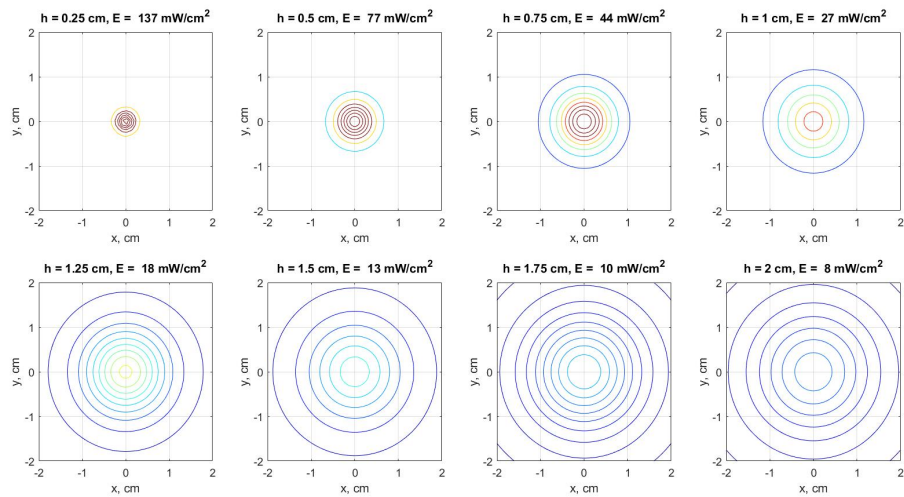


Figure 5.5: Contour plot of the variation of LED intensity: different distances (h) of the surface and the corresponding maximum of irradiance (E), CASE 1a.

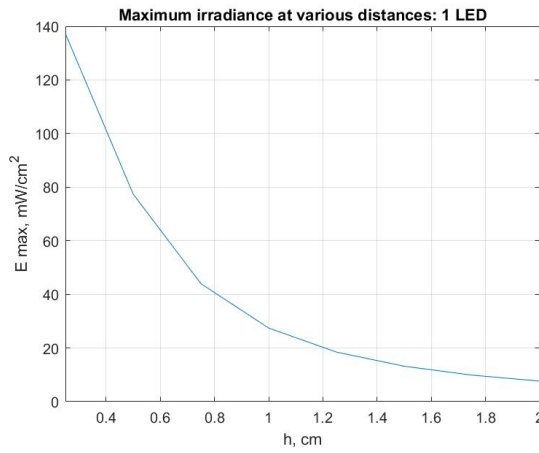
It is noticeable that the maximum of irradiance, E, reaches higher values only in proximity of the source and results decreasing at greater distances (Fig. 5.4, 5.5).

The percentage decrease has been then calculated between each subsequent distance, considering the first measurement the one made at the shortest distance of 0.25 cm (Tab. 5.2).

Table 5.2: Percentage decrease at each step d , Case 1a.

Decrease (%)	d_{2-1}	d_{3-2}	d_{4-3}	d_{5-4}	d_{6-5}	d_{7-6}	d_{8-7}	d_{tot}
Case 1a	43.8	42.8	38.6	33.3	27.7	23.1	20.0	94.2

The irradiance trend of a single source-LED has been represented in Fig.5.6: to each distance of the surface from the source corresponds its matching irradiance distribution and the resulting value in Tab. 5.2 show a degrowth of about 20% at each step, with a total percentage reduction of 94.2 % from 0.25 cm ($E = 137 \text{ mW/cm}^2$) to 2 cm ($E = 8 \text{ mW/cm}^2$).

**Figure 5.6:** Distance-dependence of 1 LED irradiance, CASE 1a.

5.2.2 Validation

TracePro®, a commercial ray-tracing software, has been used to validate the LED source of the developed simulation code.

Referring to Figure 5.7, the first grey-plane, contains the yellow LED, whereas the second surface, in green, is the moving surface, $h = 0 \text{ cm}$ to 2 cm , on which irradiance is displayed at various distances; its material has been set as a perfect transmitter. The parameters of the LED source have been set as shown in Fig. 5.9, choosing the “*Lambertian*” angular distribution and setting the incidence Flux at 0.1 W ($= 100 \text{ mW}$), as for CASE 1a. After having selected, for continuity with respect to the simulation code, to evaluate the maximum irradiance on the surface h at a distance of 1 cm from the source, the “*Trace Rays*” is displayed as reported in Fig. 5.8.

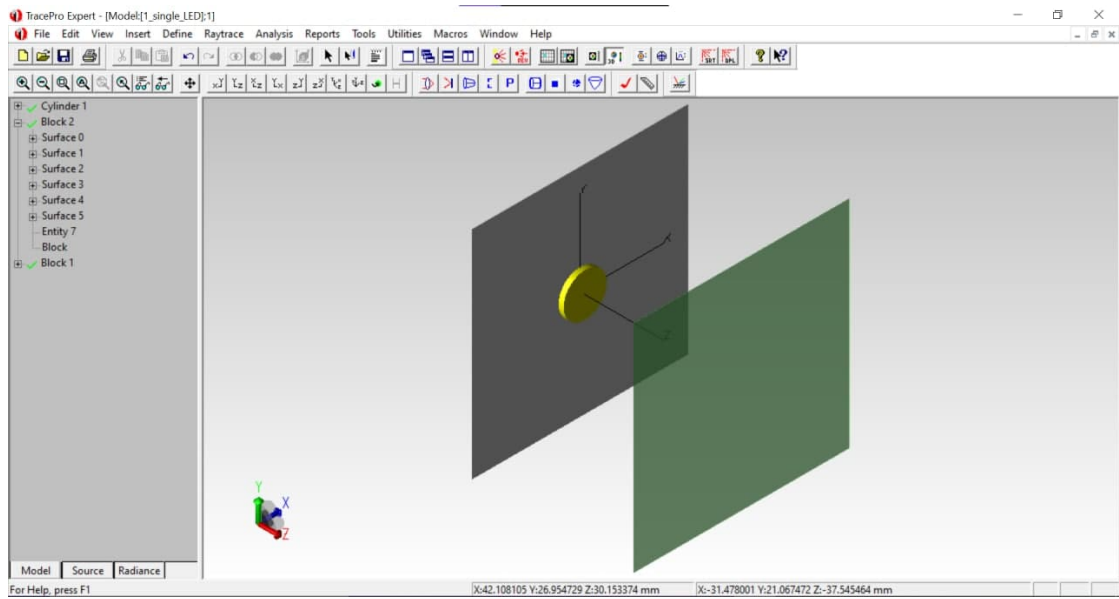


Figure 5.7: Initial model: LED (yellow) on a plane $4 \times 4 \text{ cm}$ and that distant 2 cm from the target surface.

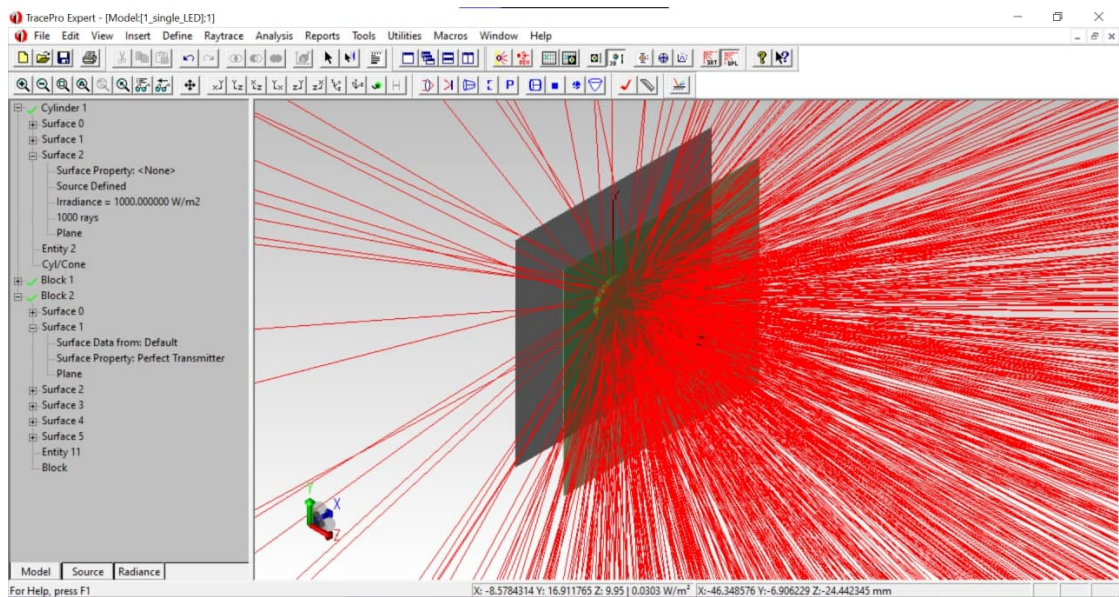


Figure 5.8: LED-ON distant 1 cm from the target surface.

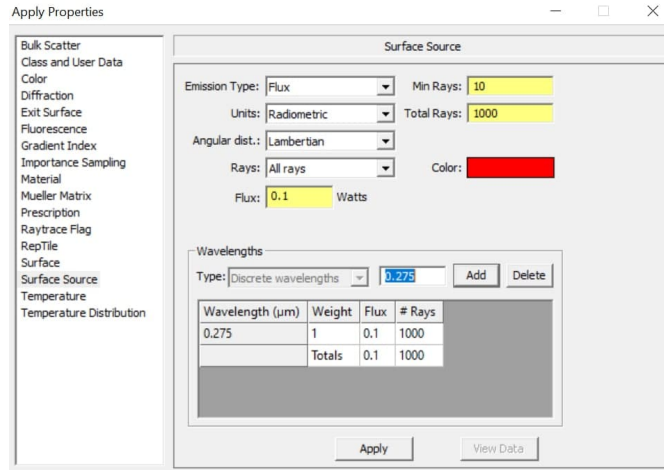


Figure 5.9: Parameters set for the LED source.

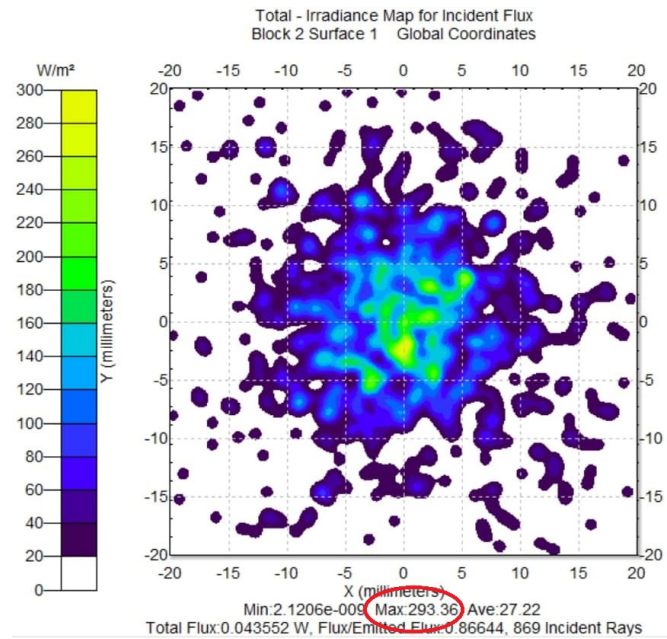


Figure 5.10: Irradiance Map: CASE 1a.

On the selected surface, the *Irradiance Map* of the incident flux is showed (Fig. 5.10): in the caption below the *TracePro* illustration, in addition to other values, the maximum of irradiance is reported. The value is of 29.33 mW/cm² for the validation system and it corresponds to the 27.43 mW/cm² in the implemented one, for CASE 1a, with a result accuracy of 93.5% of the implemented code.

5.3 Different sources on a plane

Several geometries have been experimented and discussed to find the best that offers great values in term of sufficient homogeneously irradiance supply. Infinite are the possible combinations of LEDs. The following basic combinations have been chosen to study a simplified model composed of two or four LEDs on the same plane.

5.3.1 CASE 2a

2 LEDs

In this configuration the modified variables are:

- coordinates: $P_1 (0.5,0)$ and $P_2(-0.5,0)$,
- distance: $h = 0.5$ cm,
- distance inter-LED = 1 cm.

It has been chosen contour plot and pseudo-color plot of the irradiance of the two sources on a surface placed at 0.5 cm as it can better visualize the shape of the configuration (Fig. 5.11). Variations of irradiance have been represented in the same range 0.25 cm to 2 cm, like the previous case, in Figure 5.12. The same general irradiance trend can be seen, but with enhanced values due to the both contributes.

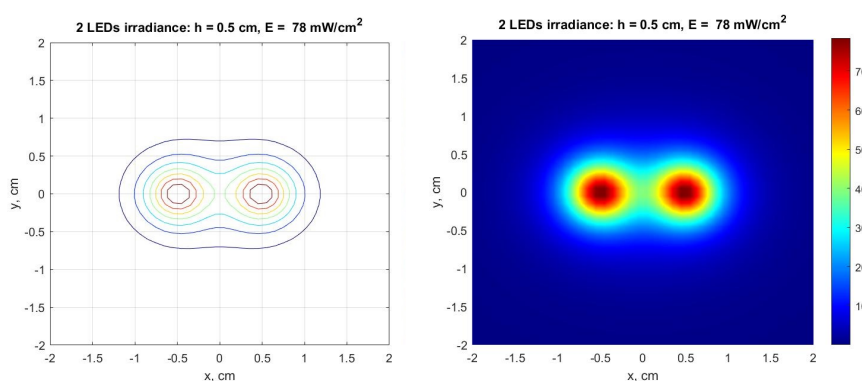


Figure 5.11: Contour plot and pseudo-color representation of irradiance, in a surface with $h = 0.5$ cm, with coordinates $P_1(0.5,0)$, $P_2(-0.5,0)$, CASE 2a.

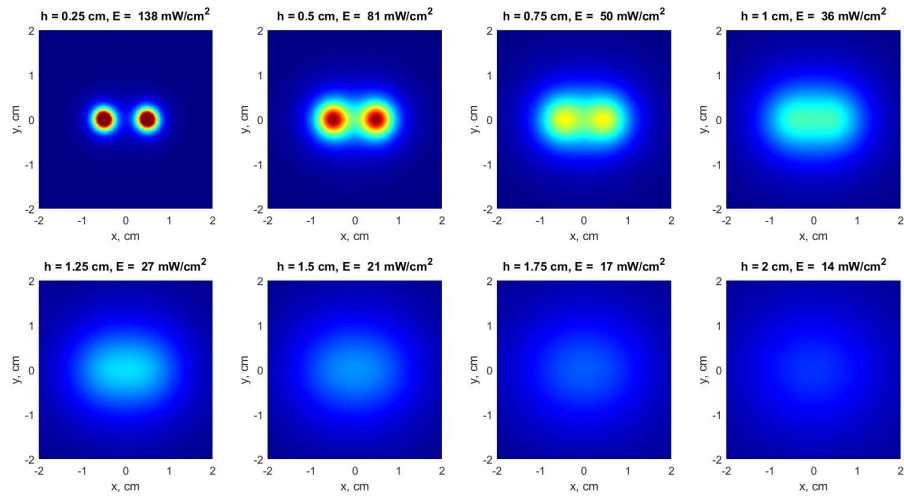


Figure 5.12: Pseudo-color plot of the variation of LEDs intensity: different distances (d) of the surface and the corresponding maximum of irradiance (E), CASE 2a.

The graphic below shows the same dependence of the light intensity with the distance of the considered surface: the total decrease from the lowest distance ($E = 138 \text{ mW/cm}^2$) to the highest one ($E = 14 \text{ mW/cm}^2$) of the irradiance is of 89.8% (Fig. 5.13) with a smaller decrease along the various propagation distances than the respective results of the previous case (Tab. 5.4).

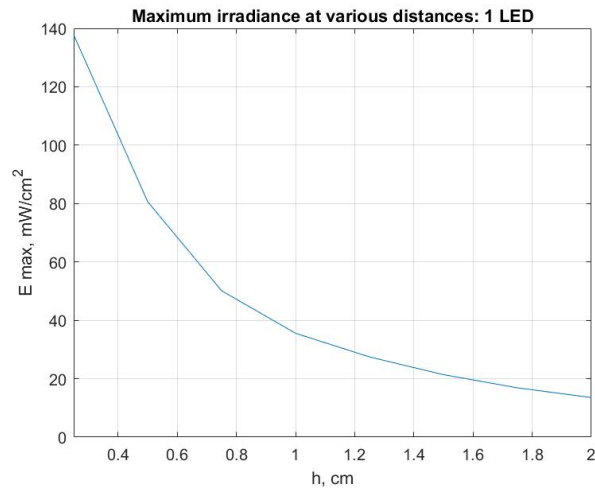


Figure 5.13: Distance-dependence of 2 LEDs irradiance, CASE 2a.

Table 5.3: Maximum of irradiance at different distances h , Case 2a.

Maximum of irradiance (mW/cm ²)	h_1	h_2	h_3	h_4	h_5	h_6	h_7	h_8
Case 2a	138	81	50	36	27	21	17	14

Table 5.4: Percentage decreases at each step d , Case 2a.

Decrease (%)	d_{2-1}	d_{3-2}	d_{4-3}	d_{5-4}	d_{6-5}	d_{7-6}	d_{8-7}	d_{tot}
Case 2a	41.3	38.3	28.0	25.0	22.2	19.0	17.0	89.9

5.3.2 CASE 3a

4 LEDs in line

This LED configuration is composed of 4 LEDs, positioned on the same horizontal line, and separated from the next nearest of 0.5 cm, (Fig. 5.14). It has been chosen this distance because, by considering Case 2a, it has been seen that a shorter separation between sources might lead to better results, due to an enhanced sum of intensities. In this configuration the modified variables are:

- coordinates: $P_1(-0.75,0)$, $P_2(-0.25,0)$, $P_3(0.25,0)$, $P_4(0.75,0)$,
- distance: $h = 0.5$ cm,
- distance inter-LED = 0.5 cm.

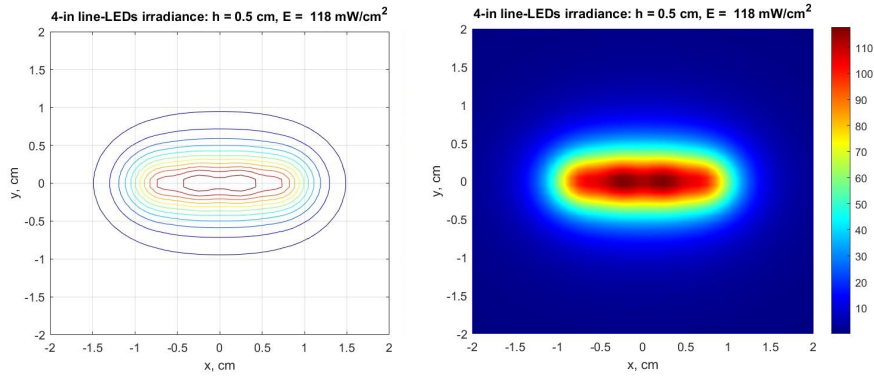


Figure 5.14: Contour plot and pseudo-color representation of irradiance, in a surface with $h = 0.5$ cm, with coordinates $P_1(-0.75,0)$, $P_2(-0.25,0)$, $P_3(0.25,0)$, $P_4(0.75,0)$, CASE 3a.

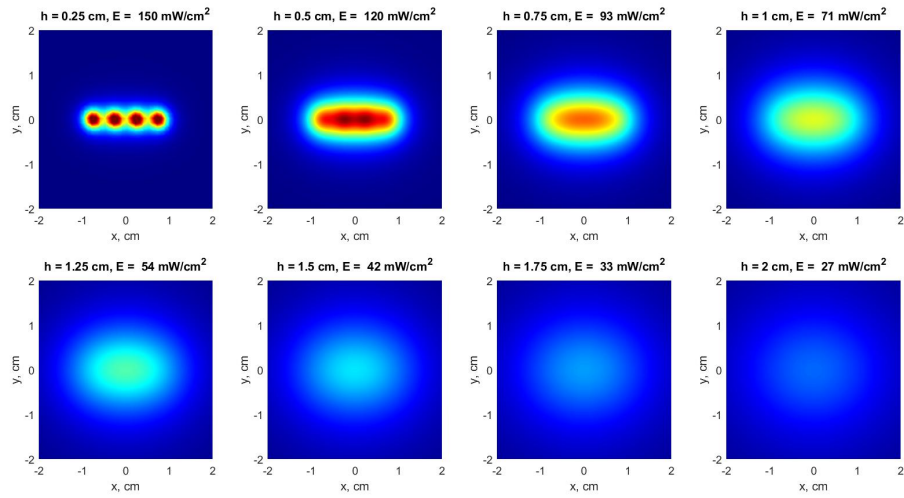


Figure 5.15: Pseudo-color plot of the variation of LEDs intensity: different distances (d) of the surface and the corresponding maximum of irradiance (E), CASE 3a.

Table 5.5: Maximum of irradiance at different distances h , Case 3a.

Maximum of irradiance (mW/cm^2)	h_1	h_2	h_3	h_4	h_5	h_6	h_7	h_8
Case 3a	150	120	93	71	54	42	33	27

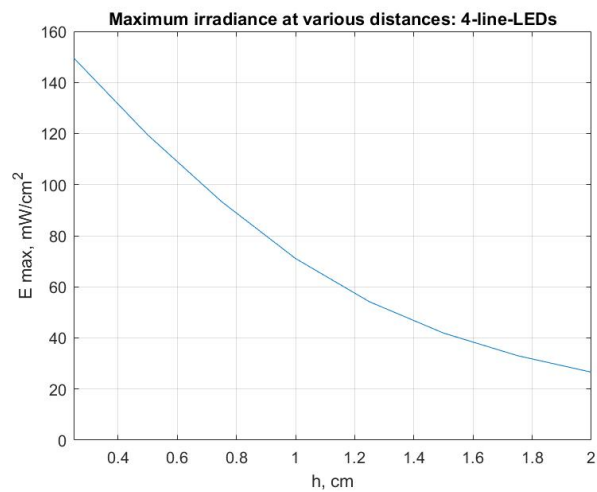


Figure 5.16: Distance-dependence of 4-in-line-LEDs irradiance, CASE 3a.

Table 5.6: Percentage decreases at each step d , Case 3a.

Decrease (%)	d_{2-1}	d_{3-2}	d_{4-3}	d_{5-4}	d_{6-5}	d_{7-6}	d_{8-7}	d_{tot}
Case 3a	20.0	22.5	23.6	31.5	22.2	21.4	18.2	82.0

For this configuration different explanations can be exposed by observing the percentage decreases in Tab. 5.6: in the first two previous cases the irradiance at the minimum distance was similar, showing a linear decrements in the following measurements. With 4 LED in-line, instead, a slower decrease has been verified to short distances, if compared to the respective values of the other cases. Thus, this geometry has appeared to be more performing for the higher irradiance and for the major uniformity of intensity distribution also confirmed by the lower total decrease of 82%. Cumulative effect of LEDs in nearby positions is verified for shorter distances, under 1.25 cm.

5.3.3 CASE 4a

4 LEDs in a square of 1 cm side

Among all the possible imaginable configurations, the square has been selected (Fig. 5.17). This geometry has been made of 4 LEDs, each one is at the vertices of a square of side 1 cm, same LED values have been adopted and the new variables are:

- coordinates: $P_1(-0.5,0.5)$, $P_2(-0.5,-0.5)$, $P_3(0.5,0.5)$, $P_4(0.5,-0.5)$,
- distance inter-LEDs = 1 cm.

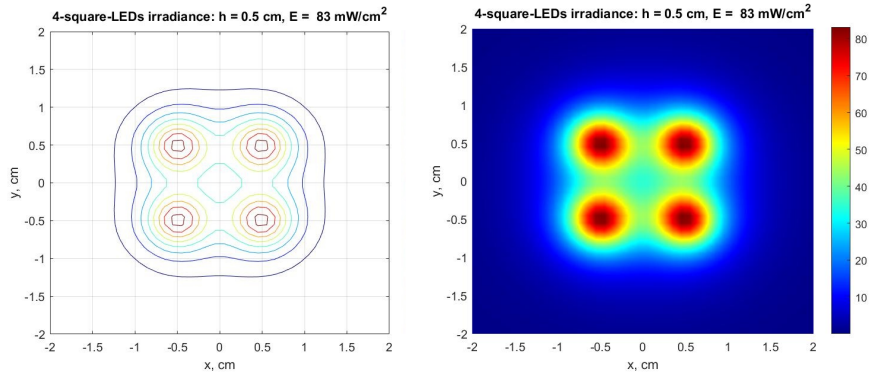


Figure 5.17: Contour plot and pseudo-color representation of irradiance, in a surface with $h = 0.5$ cm, with coordinates $P_1(-0.5,0.5)$, $P_2(-0.5,-0.5)$, $P_3(0.5,0.5)$, $P_4(0.5,-0.5)$, CASE 4a.

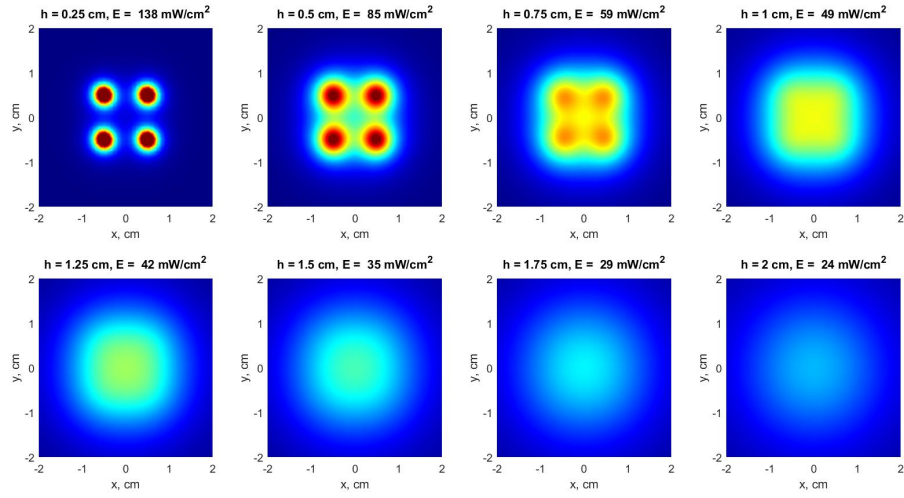


Figure 5.18: Pseudo-color plot of the variation of LEDs: different distances (d) of the surface and the corresponding maximum of irradiance (E), CASE 4a.

Table 5.7: Maximum of irradiance at different distances h, Case 4a.

Maximum of irradiance (mW/cm ²)	h_1	h_2	h_3	h_4	h_5	h_6	h_7	h_8
Case 4a	138	85	59	49	42	35	29	24

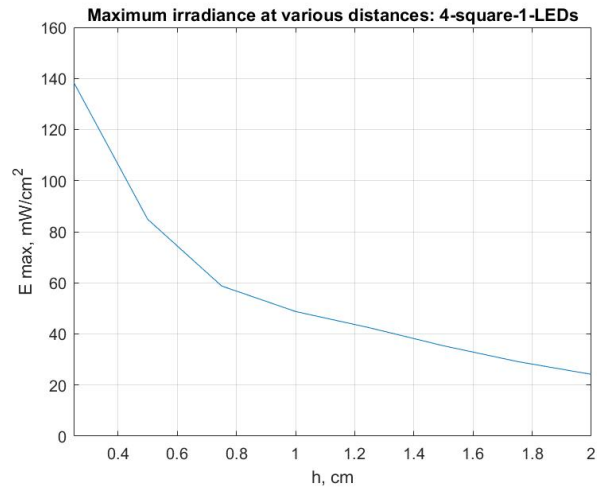


Figure 5.19: Distance-dependence of 4 LEDs irradiance, square of 1 cm, CASE 4a.

Table 5.8: Percentage decreases at each step d, Case 4a.

Decreases (%)	d_{2-1}	d_{3-2}	d_{4-3}	d_{5-4}	d_{6-5}	d_{7-6}	d_{8-7}	d_{tot}
Case 4a	38.4	30.6	16.9	14.3	16.6	17.1	17.2	82.6

In this case there are no relevant differences if compared with CASE 2a for the initial percentage decrease: 138 mW/cm^2 and 25 mW/cm^2 are, respectively, the highest and the lowest values, with a final reduction of 82.6%, similar to CASE 3a. A particularly slow reduction in intensity has occurred in the middle part of the observation range, although the initial values do not appear to be very different from the 2-LED configuration, despite being twice as large. This result suggested a further test, bringing LEDs a little closer.

5.3.4 CASE 5a

4 LEDs in a square of 0.5 cm side

The last configuration geometry of a 4 LEDs disposition at the vertex of a square which side is 0.5 cm. The geometry is the same as Case 4a, but in this situation is has been chosen a shorted inter-LEDs distance (Fig. 5.20). The new set values are:

- coordinates: $P_1(-0.5,0.5)$, $P_2(-0.5,-0.5)$, $P_3(0.5,0.5)$, $P_4(0.5,-0.5)$,
- distance inter-LEDs = 0.5 cm.

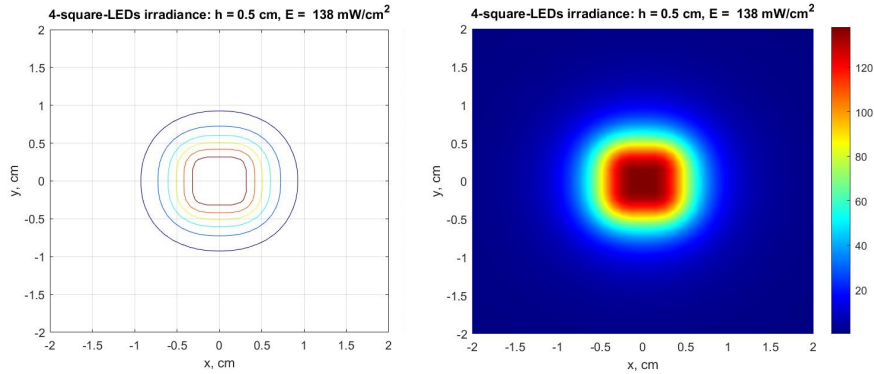


Figure 5.20: Contour plot and pseudo-color representation of irradiance, in a surface with $h = 0.5 \text{ cm}$, with coordinates $P_1(-0.25,0.25)$, $P_2(-0.25,-0.25)$, $P_3(0.25,0.25)$, $P_4(0.25,-0.25)$, CASE 5a.

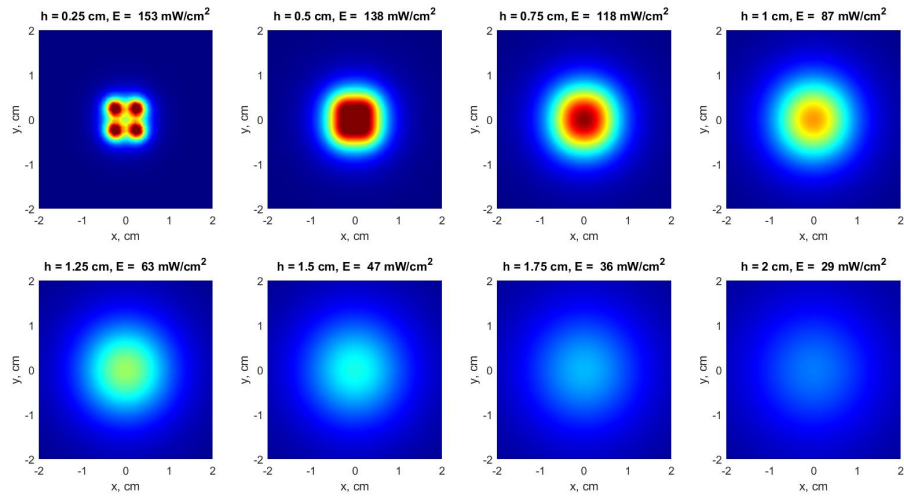


Figure 5.21: Pseudo-color plot of the variation of LEDs: different distances (d) of the surface and the corresponding maximum of irradiance (E), CASE 5a.

Table 5.9: Maximum of irradiance at different distances h, Case 5a.

Maximum of irradiance (mW/cm^2)	h_1	h_2	h_3	h_4	h_5	h_6	h_7	h_8
Case 5a	153	138	118	87	63	47	36	29

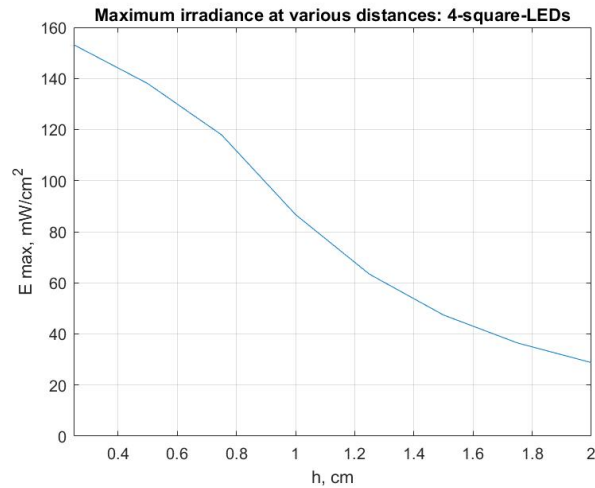


Figure 5.22: Distance-dependence of 4 LEDs irradiance, square of 0.5 cm, CASE 5a.

Table 5.10: Percentage decreases at each step d, Case 5a.

Decrease (%)	d ₂₋₁	d ₃₋₂	d ₄₋₃	d ₅₋₄	d ₆₋₅	d ₇₋₆	d ₈₋₇	d _{tot}
Case 5a	9.8	14.5	26.3	27.6	25.4	23.4	19.4	81.0

5.3.5 Comparison of the 5 CASES a

In Figure 5.11 the comparison of the irradiance values of all the performed tests in this first part, on a single plane, is reported: visually, the green and yellow curves, respectively of CASE 5a and CASE 3a provide better irradiance values. Furthermore, it can be seen that the initial slope of these two configurations decreases less quickly when compared to the other geometries. This result can also be seen in the Table 5.12, where the initial percentage decreases of the two cases (3a and 5a) have much lower values than the others. Thus, the homogeneity in the propagation is better reached with these two configurations, confirmed also with their total percentage decrease. Apart from the two better cases, the following good one is the CASE 4a: despite its initial lower value of irradiance, it shows an acceptable total trend, with a total percentage reduction of 82.6%.

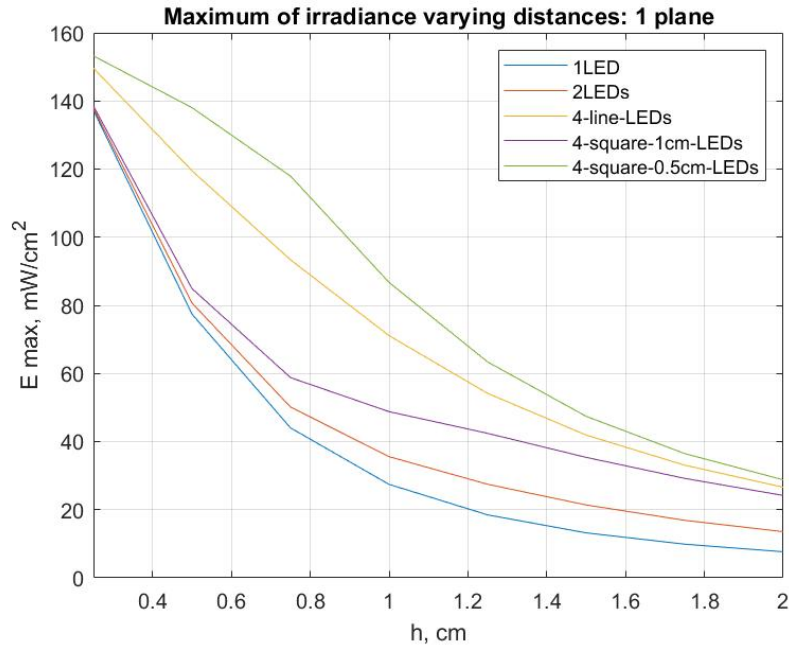


Figure 5.23: Comparison of the distance-dependence of irradiance of the treated Cases a.

In general, it can be said that the performance is improved by adding more LED sources and by bringing them closer, but everything depends on the target of the light-treatment and the associated minimum effective dose: also the worst configuration can be adopted if long exposure times are allowed. Some examples of different time exposure have been evaluated.

Table 5.11: Maximum of irradiance at different distances h , Cases a.

Maximum of irradiance (mW/cm ²)	h_1	h_2	h_3	h_4	h_5	h_6	h_7	h_8
Case 1a	137	77	44	27	18	13	10	8
Case 2a	138	81	50	36	27	21	17	14
Case 3a	150	120	93	71	54	42	33	27
Case 4a	138	85	59	49	42	35	29	24
Case 5a	153	138	118	87	63	47	36	29

Table 5.12: Percentage decreases at each step d , Cases a.

Decrease (%)	d_{2-1}	d_{3-2}	d_{4-3}	d_{5-4}	d_{6-5}	d_{7-6}	d_{8-7}	d_{tot}
Case 1a	43.8	42.8	38.6	33.3	27.7	23.1	20	94.2
Case 2a	41.3	38.3	28.0	25.0	22.2	19.0	17.0	89.9
Case 3a	20.0	22.5	23.6	31.5	22.2	21.4	18.2	82.0
Case 4a	38.4	30.6	16.9	14.3	16.6	17.1	17.2	82.6
Case 5a	9.8	14.5	26.3	27.6	25.4	23.4	19.4	81.0

Examples of different required exposure times

A realistic sanitation situation has been proposed to evaluate the solution that provides the best results, using as test values a required dose D of 6.6 mJ/cm², used in literature for the inactivation of *E.coli*, and the exposure times of $t_1=0.07$ s, $t_2=0.1$ s, $t_3=0.5$ s (Fig. 5.24). If the disinfection system would be used in short exposure times, as for the cases of t_1 and t_2 , the only two recommended configurations to be used, at no too greats distances, are that of CASE 3a and CASE 5a, “4 in-line LEDs” and “4-square-0.5cm-LEDs” respectively. However, if sanitization may require longer irradiation times, the other configurations are also appropriate.

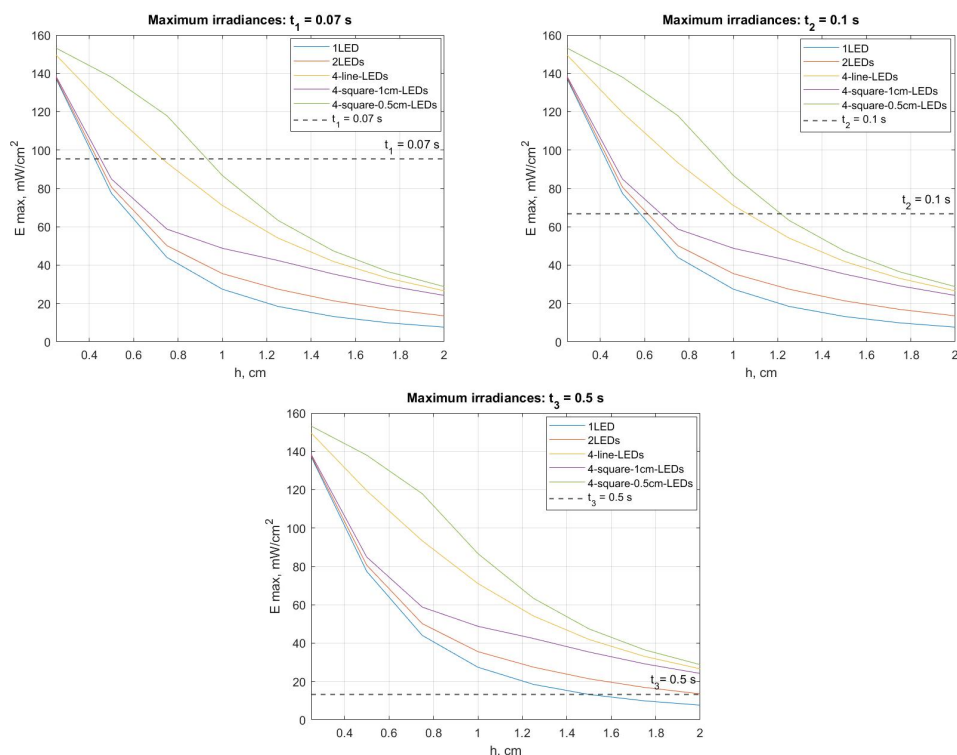


Figure 5.24: Comparison between the three exposure times, CASES a.

5.4 Different sources on two parallel planes

At this step, a new plane containing new sources has been added. It is equal and parallel to the plane of the previous cases, $4 \times 4 \text{ cm}$ and the distance between them is of 2 cm . The idea has come up because it has been thought to apply frontally positioned LED-sources and to verify if the delivered irradiance would provide an enhanced effect through the space between the two planes or not. Five cases, the same as before, have been treated in the similar way. For each case, coordinates of the sources are unchanged and mirrored, on both planes, to test the summation light effect and to analyze differences with the previous studies. Even if advantageous configurations have already been found, the study of the less successful cases in this geometry has also been evaluated. An initial minimum evaluation distance of 0.25 cm has been set also for the second plane, so the range of variation is from 0.25 cm to 1.75 cm .

5.4.1 CASE 1b

1 LED per plane

Coordinates are $P_1(0,0)$.

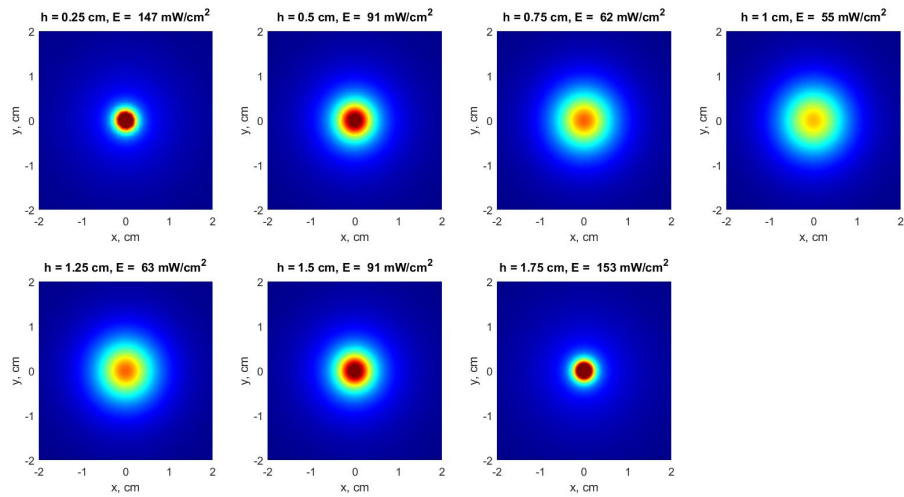


Figure 5.25: Pseudo-color plot of the variation of LED intensity: different distances (d) of the surface and the corresponding maximum of irradiance (E), CASE 1b.

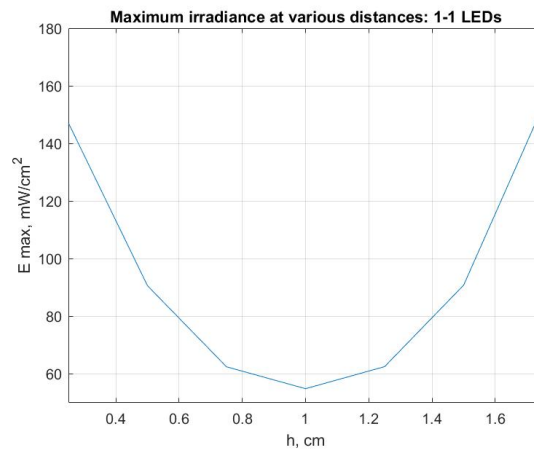


Figure 5.26: Distance-dependence of 1 LED irradiance, CASE 1b

5.4.2 CASE 2b

2 LEDs per plane

Coordinates are: $P_1(0.5,0)$, $P_2(-0.5,0)$.

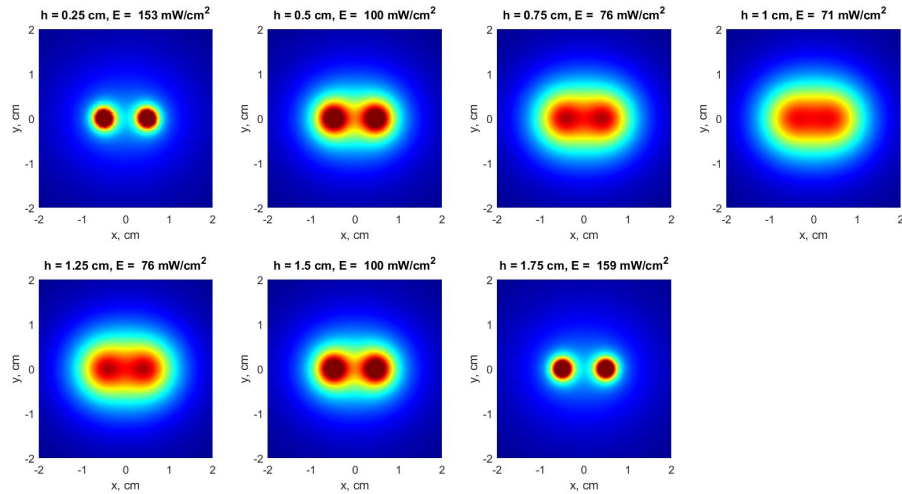


Figure 5.27: Pseudo-color plot of the variation of LEDs: different distances (d) of the surface and the corresponding maximum of irradiance (E), CASE 2b.

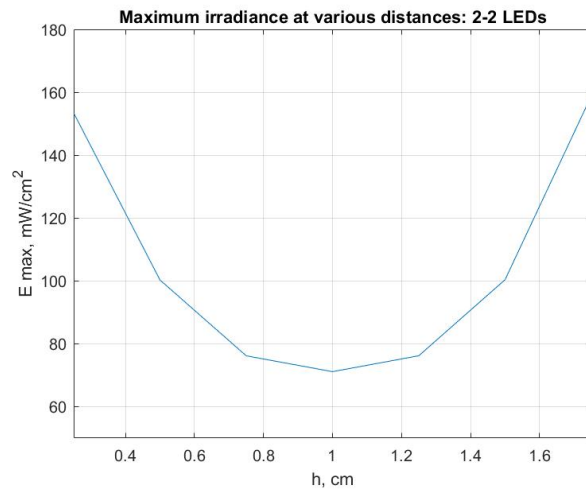


Figure 5.28: Distance-dependence of 2 LEDs irradiance, CASE 2b.

5.4.3 CASE 3b

4 LEDs in line, per plane

Coordinates are: $P_1(-0.75,0)$, $P_2(-0.25,0)$, $P_3(0.25,0)$, $P_4(0.75,0)$.

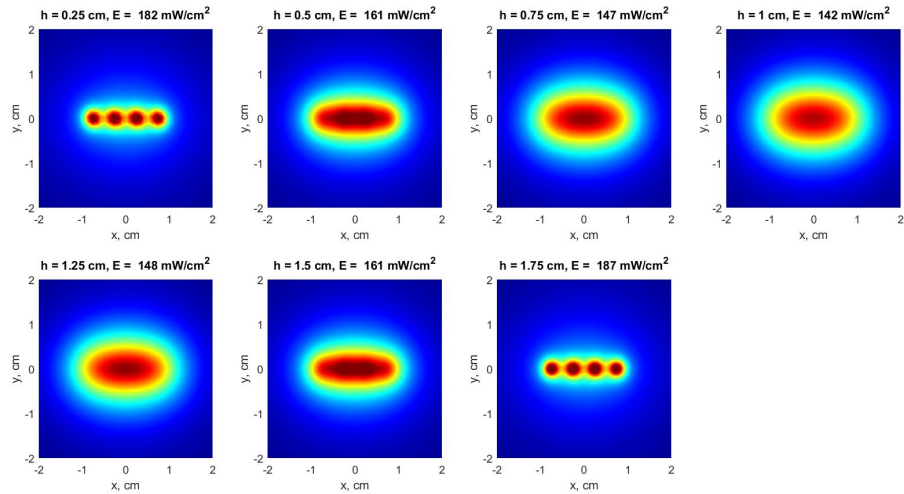


Figure 5.29: Pseudo-color plot of the variation of LEDs: different distances (d) of the surface and the corresponding maximum of irradiance (E), CASE 3b.

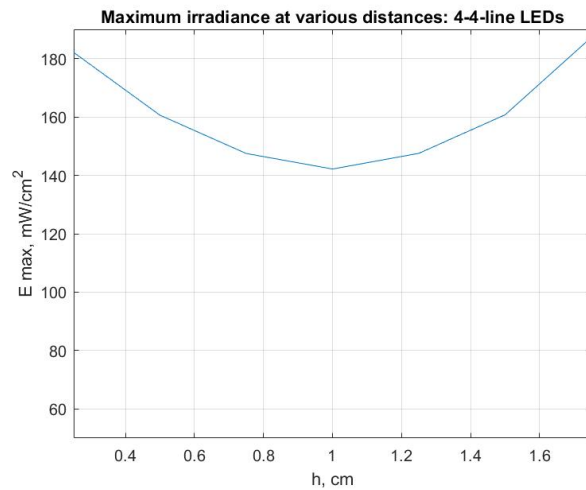


Figure 5.30: Distance-dependence of 4-in-line-LEDs irradiance, CASE 3b.

5.4.4 CASE 4b

4 LEDs in a square of 1 cm side, per plane

Coordinates are: $P_1(-0.5,0.5)$, $P_2(-0.5,-0.5)$, $P_3(0.5,0.5)$, $P_4(0.5,-0.5)$.

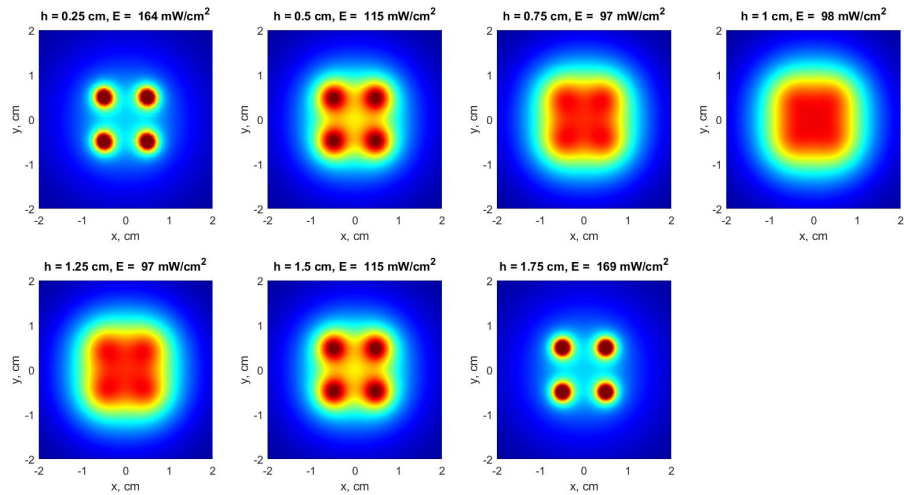


Figure 5.31: Pseudo-color plot of the variation of LEDs: different distances (d) of the surface and the corresponding maximum of irradiance (E), CASE 4b.

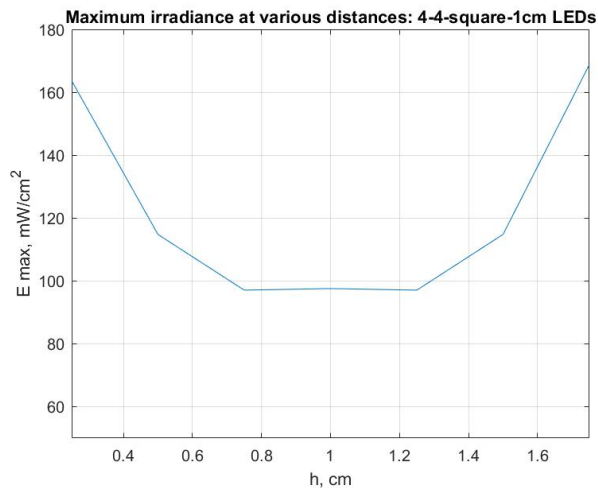


Figure 5.32: Distance-dependence of 4 LEDs irradiance, square of 1 cm, CASE 4b.

5.4.5 CASE 5b

4 LEDs in a square of 0.5 cm side, per plane

Coordinates are: $P_1(-0.25,0.25)$, $P_2(-0.25,-0.25)$, $P_3(0.25,0.25)$, $P_4(0.25,-0.25)$.

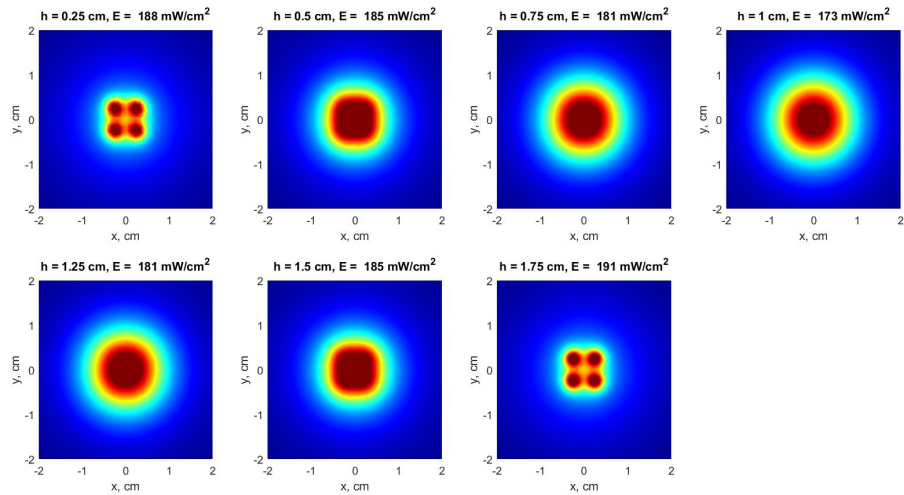


Figure 5.33: Pseudo-color plot of the variation of LEDs: different distances (d) of the surface and the corresponding maximum of irradiance (E), CASE 5b.

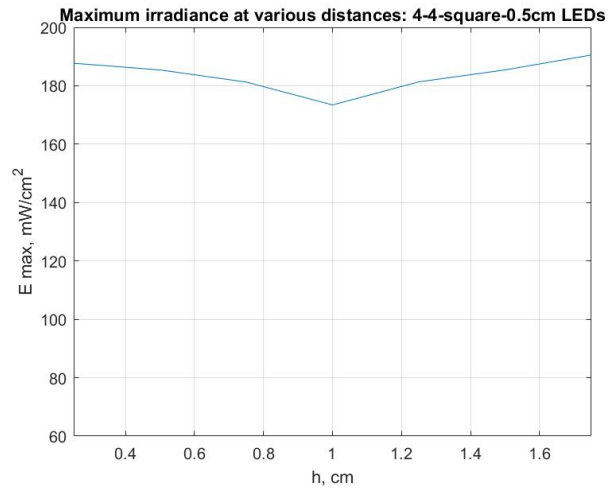


Figure 5.34: Distance-dependence of 4 LEDs irradiance, square of 0.5 cm, CASE 5b.

5.4.6 Comparison of the 5 CASES b

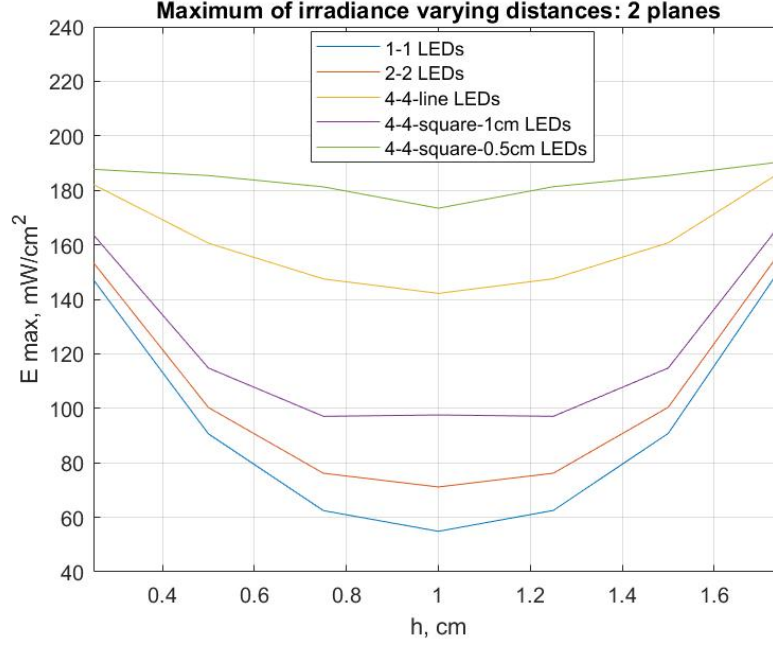


Figure 5.35: Comparison of the distance-dependence of irradiance of the treated Cases b, $\phi_e = 100$ mW.

Table 5.13: Maximum of irradiance at different distances h, Cases b.

Maximum of irradiance (mW/cm ²)	h_1	h_2	h_3	h_4	h_5	h_6	h_7
Case 1b	147	91	62	55	63	91	153
Case 2b	153	100	76	71	76	100	159
Case 3b	182	161	147	142	148	161	187
Case 4b	164	115	97	98	97	115	169
Case 5b	188	185	181	173	181	185	191

This second set of configurations, CASES b, as already said, have been created by mirroring the two planes with their respective LEDs. For this reason, it was expected to find near both surfaces the same maxima of irradiance, decreasing towards the central part of the structure. Due to this explanation, confirmed with the Figure 5.35 and the trend of each Case b described in Table 5.13, the

Table 5.14: Percentage decreases at each step d , Cases b.

Decreases (%)	d_{2-1}	d_{3-2}	d_{4-3}	d_{tot}
Case 1b	38.1	31.8	11.3	62.3
Case 2b	34.6	24.0	6.5	53.6
Case 3b	11.5	8.7	3.4	21.9
Case 4b	29.8	15.6	1.0	40.0
Case 5b	1.6	2.1	4.4	7.9

percentage reductions have been calculated only for the first half of the considered distances. The best geometries are Case 3b with a value of 21.9% and that of the Case 5b, with the minimum total percentage decrease of 7.9%. The corresponding percentage reduction, in the half distance, of Cases a are of 52.3% (3a) and 22.8% (5a), so a more penetrating solution is the frontal addition of a second plane of sources.

Examples of different required exposure times

In addition to the three exposure times previously used to evaluate operating effectiveness, $t_1=0.07$ s, $t_2=0.1$ s, $t_3=0.5$ s, a fourth is added, $t_4=0.04$ s; it is the minimum time value that can be analyzed for at least one of the configurations to be adequate, that of Case 5b. Comparing these results to those of Fig. 5.24, it can be said that, for $t_1=0.07$ s, in Cases a only 2 configurations were able to provide the sufficient irradiation to the 40% of the depth, whereas in this Cases b, 3 of them cover the totality of the considered distances; same observation can be exposed for $t_2=0.1$ s, in which almost all the configuration are adequate for the hole space for Cases b, respect to the 2 (3a and 5a) that covered the 60% and the others with an action only on the 30%. For prolonged times, $t_3=0.5$ s, results are similar, while only these Cases b are applicable for smaller sanitization times $t_4=0.04$ s.

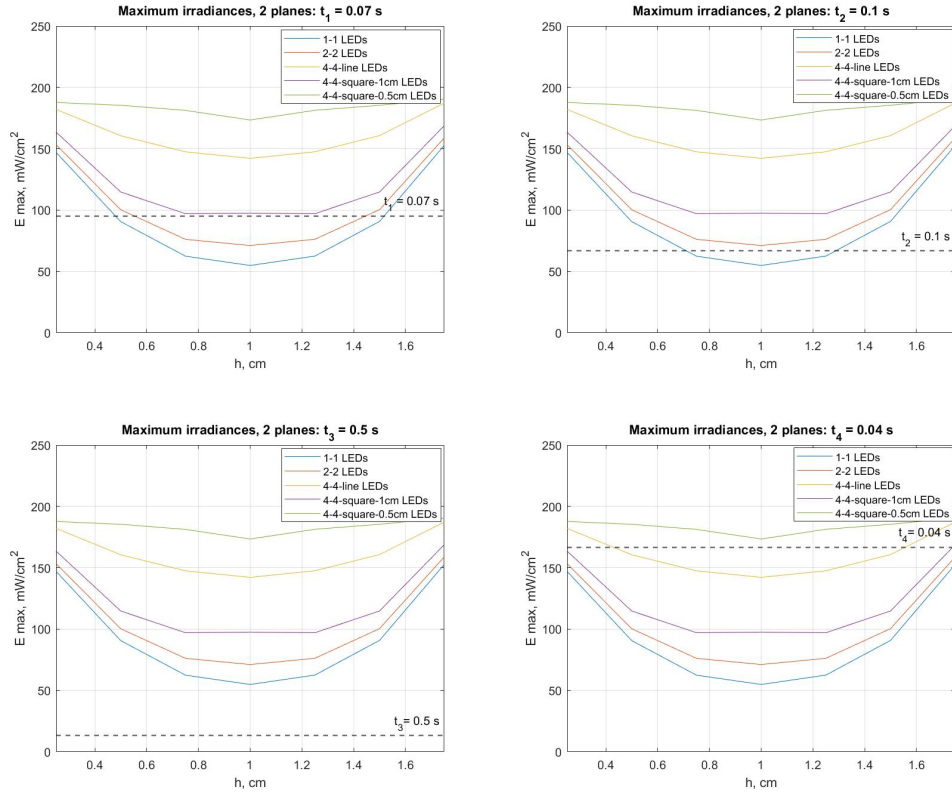


Figure 5.36: Comparison between the four exposure times, CASES b.

5.5 Aluminum Structure

In this section of the work, other considerations have been made on the material of the developed two-parallel-system: the idea is to use it for water sanitization, so a future development could be a tube in which flows contaminated water. The learned LED behaviour, with the greater irradiance nearby the source and a fast and strong reduction in intensity moving away from it, has suggested the use of materials with high reflective behavior that could increase the effect of light propagation. Metals have been chosen for their high reflectivity, the property that a surface has of reflecting incident radiation upon it. The reflectance parameters are empirical values depending on the used material and the wavelength of radiation that invests it. Aluminum reflectance have been involved because of considerable impact (over 70-80%) along the nanometer and micrometer wavelengths, acting almost like a mirror: in this simulation, it has been selected a value of 70%, which corresponds to the reflectivity of aluminum at 275 nm [39]. This feature is supposed to enhance the irradiance values obtained and to improve the performance of the system.

The implementation of the code previously used for the examined cases has been

performed, adding the contribution of reflectance to then evaluate the eventual differences.

The first part of the MATLAB® code for the representation of the aluminum system consists in the implementation of Eq. 5.10 to simulate the Lambertian source and the emitted irradiance, as it has been done before. In the second part the aluminum reflection has been implemented through the steps below:

- The total irradiances coming from every plane have been evaluated at different distances, among the width of the structure.
- It is assumed that each ray can be reflected multiple times. The first reflection has been created considering the incident radiation on the opposite aluminum surface and multiplying it for the corresponding Aluminum reflectance for the selected wavelength.
- After the first reflection, multiple rays reflections have been added; the mirroring effects continue until the values of the reflected irradiance tends to zero (0.01). This assumption does not consider losses and dissipations since it tries to approach the simplified simulation of a structure that is delimited by two planes of aluminum, forming together to the two just described, a structure of a square base tube. In such case, ulterior modifications to the code would have to be carried out.
- Total contributions are added up for each distance.

5.5.1 Discussion

This study has therefore been used to evaluate the incidence of the use of the aluminum material on the resulting distribution of irradiance between the two flat surfaces. The five Cases-b have been compared together before and after the application of the reflectance. From Fig. 5.37 and Fig. 5.38. it can be seen that aluminum has provided a significant contribution to the results previously obtained. In addition, in Table 5.15, the percentage increases of averaged irradiances of each configuration following the addition of the reflectance factor have been reported.

To conclude, it has emerged that the reflectance factor of a metallic material adds a clear contribution to the performance of the LED system tested: it can be seen that, for short exposure times ($t_4=0.04$ s), it provides a sufficiently adequate distribution even in less performing configurations composed of a lower number of LEDs, optimizing costs and consumption of electronics employed and facilitating the antimicrobial action of the system.

Future developments could concern the study of a closed structure, for instance cylindrical in shape, composed of materials with different indexes of reflections, to evaluate differences in order to make the system integrate in hydraulic piping for

the supply of sanitized water. Moreover, further studies could be done evaluating the dynamics of the fluid-flow that invests the pipe, to observe in detail the behavior and to assess any phenomena that may occur along the various material interfaces.

Table 5.15: Percentage increases of Cases b after implementation with aluminum reflectance.

Cases	1b	2b	3b	4b	5b
Increases (%)	32.4	40.7	47.8	49.6	46.8

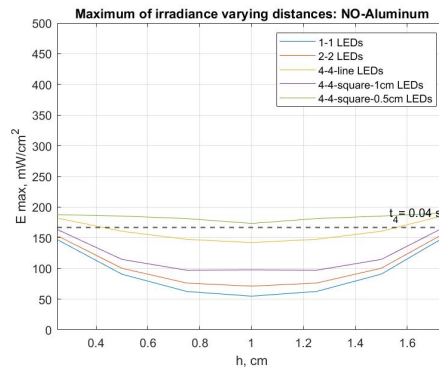


Figure 5.37: Non-Aluminum Cases b, Maximum irradiance, $t_4=0.04$ s.

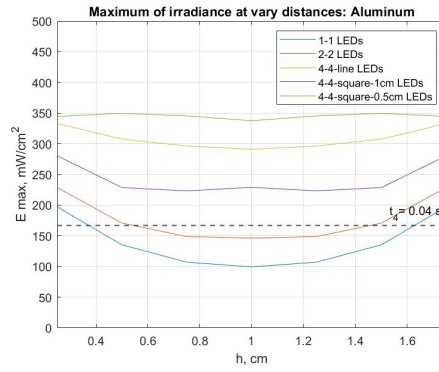


Figure 5.38: Aluminum Cases b, Maximum irradiance, $t_4=0.04$ s.

Chapter 6

Experimental Section 1: UVC and blue LEDs for water disinfection

The target of these experiments is a quantitative evaluation of the efficacy of two sources, a UVC LED and a blue LED, for the sanitation of *Enterobacteriaceae* in water. Slides for total bacterial count and *Enterobacteriaceae* detection have been employed to detect the evolution in the amount of bacteria before and after the experiments.

6.1 Circuit: UVC and blue LED

This set of experiments aims at detecting the presence of bacteria in water solutions, after irradiating with UVC and blue sources. Different sanitation times have been tested with both sources in order to understand if the synergistic effect can help in disinfection and to find the minimum dose delivered that reach the highest percentage of bacterial inactivation.

Initial considerations

Blue source alone, due to its lower energy, is known to be less used for disinfection purposes, so the first theoretical consideration to take into account is that the source UVC would require less time exposures than the 405 nm source. As seen in literature, to reach the 99% of sanitization of *Enterobacteriaceae* different doses should be applied and in this study have been selected those used in literature for *E. coli* eradication: 6.6 mJ/cm² for UVC and 108 J/cm² for blue source. The starting point for the evaluation of the exposure times to use in the experiments is

a simulation with *TracePro* (Fig. 6.1). Considering the mean of irradiances of the two sources at a distance of 1 cm, 2.7 mJ/cm^2 for the UVC source and 68 mJ/cm^2 for the blue source, the eradication of the treated bacteria should occur after 2.4 s for UVC and after 26 minutes for the blue source.

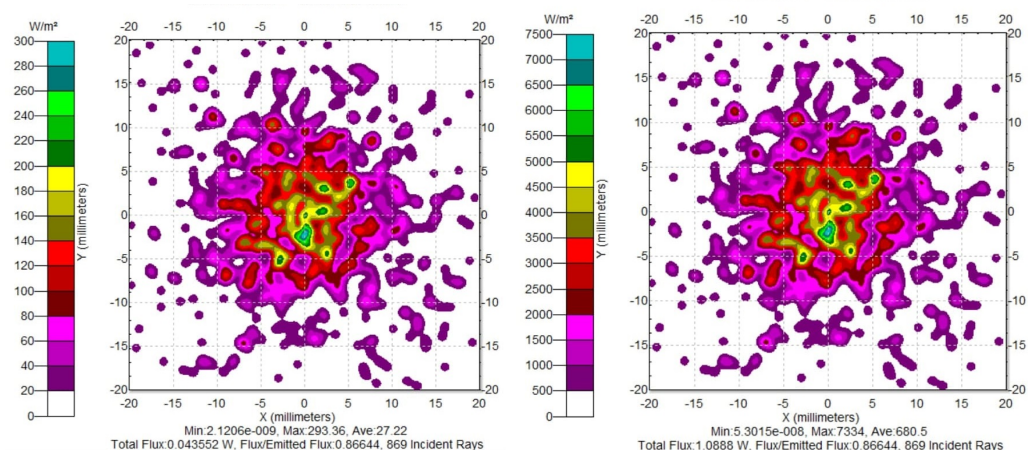


Figure 6.1: Simulations of UVC and blue LEDs with *TracePro*.

6.1.1 Material & Methods

Material used for irradiation

The used instrumentation for this experimental part is composed of: a UVC-LED at 275 nm, with optical power of 100 mW, a blue LED at 405 nm, with optical power of 2.4 W, both integrated in the same circuit. The power supply is at 24 V for both sources. There are slides for surfaces and liquids bacteriological control *Contact Slide 1*, Liofilchem®, sensitive to *Enterobacteriaceae*, the incubator *IVYX Scientific* set at a temperature of 37 °C, multi-well Petri dishes and sterilized syringes.

The set-up for UVC and blue radiation test is showed (Fig. 6.2). Almost all the experiments have been made with it: a digital caliper is used to position the height at which the circuit with the LEDs is fixed on the metal guide; to obtain the better disinfection effect, it has been selected a minimum distance of 2.5 cm from the ground. Then, the multi-well Petri dishes, filled with solution to be sanitized, have been placed under this structure.

Methods

Although every experiment has been performed with proper water concentration and time of irradiation, all tests follow the same procedure (Fig. 6.3).

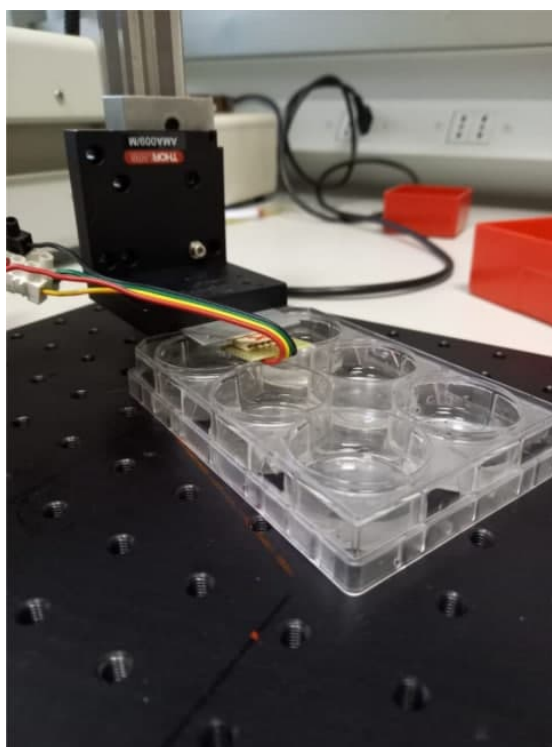


Figure 6.2: Set-up for UVC and blue LED irradiation.

The contaminated solution has been obtained by dissolving feline feces in water in a jar and then by adding it in a beaker with 250 mL of pure water. The following steps have been performed:

1. **Step 1.** The contaminated solution has been picked up with a sterile syringe and distributed into the multi-well dishes: each one is almost half filled because, as is known, UVC has a limited penetration depth, especially in liquids.
2. **Step 2.** Before irradiating, LEDs have been switched-on, without the dishes below, for approximately 10 s in order to reach the steady state of the power, overcoming the initial LED transient and to have a constant irradiance during the tests. At the same time, a first agar slide has been immersed in the beaker solution for 10 s and then placed in the incubator: this is the control medium. Then, the Petri dishes have been inserted under the sources and the sanitization process begins. In this step the irradiated solution has been manually kept in motion so as to promote homogeneous disinfection of the entire contents of each dish.
3. **Step 3.** After the exposition, the disinfected samples have been collected in a new beaker in which a new culture medium is immersed for 10 s. In some

cases the sanitized content has been directly poured on the culture medium.

4. **Step 4.** The culture medium, inserted in its tube, has been placed in the incubator at 37 °C. After 24 h, the *Contact Slide 1* have been taken out and the presence of bacterial colonies is detectable by observing the red spots on their surfaces.

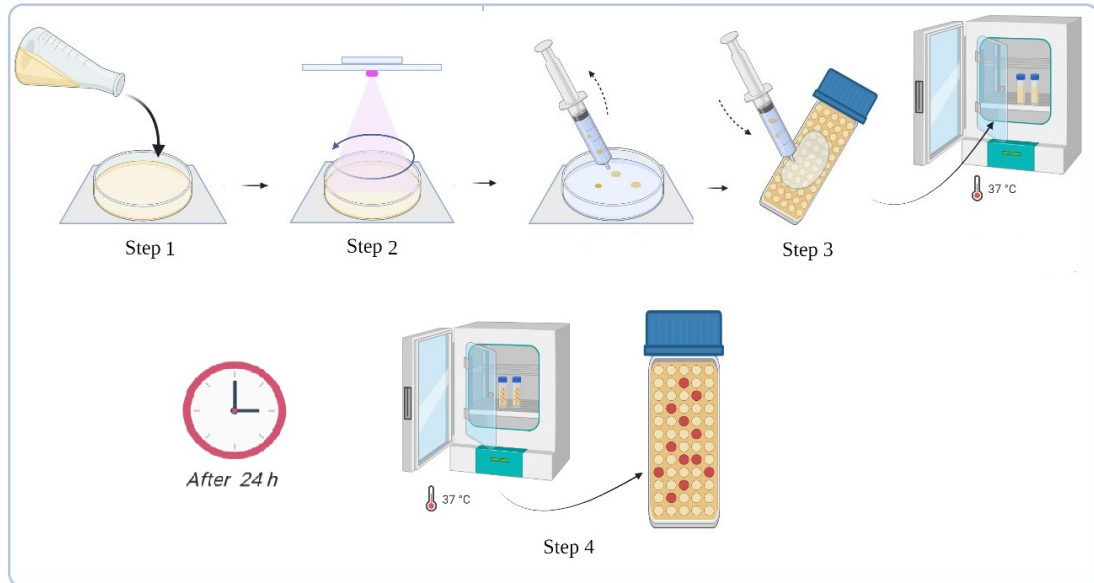


Figure 6.3: Steps of the experiments.

The following are descriptions of the three types of experiments that have been performed.

6.1.2 First set of tests

The objective is to evaluate the synergistic action of UVC-LED and blue LED. As seen from the evaluations of exposure times with *TracePro* simulations (Fig. 6.1), the germicidal effect of the 275 nm source is stronger than that of blue LED, because it is known that the major effectiveness is close to 265 nm. Even if the blue source, requiring much higher exposure times, is supposed to be almost negligible if coupled with UVC, this set of trials has been done to demonstrate the results of combining UVC radiation with blue radiation.

Data of the experiment

In this first experiment a sample of 10 mL of contaminated water has been inserted in a beaker containing 250 mL of pure water. Five *Contact Slide 1* have been used: one for the check sample, two for evaluation of the only UVC source and the rest for the combination of the two LEDs. The distance source-samples is of 25 mm and the investigated irradiation times are 3 s and 5 s.

Results

After the 24 h of incubation a visual evaluation has been made. Looking at the Figure 6.4, the first at the left is the check Slide, the the pair of tests at 3 and 5 s, in particular the forward tubes are related to UVC only irradiations while the rear ones are related to irradiations generated by the combination of both LEDs. It is possible to see a remarkable decrease of the initial bacterial load thanks to the germicidal action of the LED UVC and, above all, it can be noticed that on the agar surfaces there is no more bacterial load. However, only on one tube can be observed the growth of a colony and it is the one related to a disinfection with only UVC LED. Subsequent tests will be performed with shorter times in order to demonstrate if indeed the combined UVC+Blue action is greater than a sanitization UVC only.

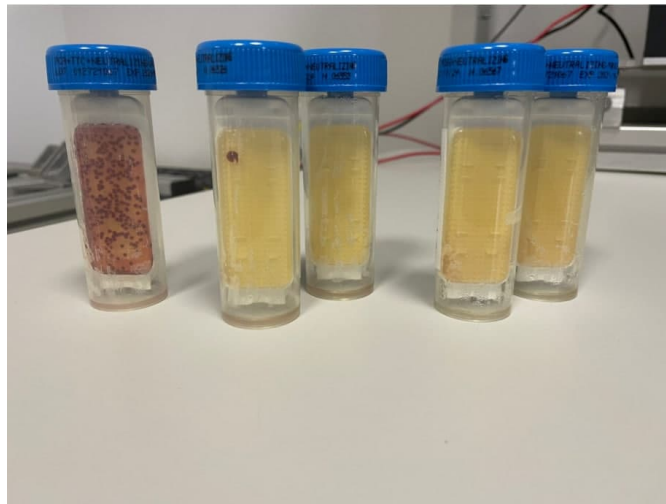


Figure 6.4: Post-exposure: experiments with 3 s and 5 s, 10 mL of contaminated water.

6.1.3 Second set of tests

To demonstrate the effectiveness of combining radiation at 405 nm with that at 275 nm, the compounds of contaminated water have been increased and the irradiation times decreased. In addition, in order to obtain a good repeatability, several tests have been performed with the same irradiation times.

Data of the experiment

A sample of 20 mL of contaminated water has been mixed with 300 mL of pure water. Seven test tubes have been used: one was used as a control sample, 3 to immerse them in the liquid disinfected with UVC radiation only and the rest were used to immerse them in the liquid disinfected by both LEDs. The irradiation time is of 2 s for all the tests.

Results

Observing Figure 6.5, the test tubes are arranged as follows: on the left there is the control sample, followed by the pair of tests at 2 s, in particular, the rear test tubes are related to UVC irradiations only, while the front ones are related to irradiations generated by the combination of both LEDs. Following the guidelines of the *Contact Slide 1* Datasheet, it can be seen that the test was successful: starting from a high concentration of bacteria (about 10^6 CFU/mL) a concentration of maximum 10^3 CFU/mL is obtained, where the action of the radiation at 405 nm caused a reduction of the growth of Enterobacteriaceae colonies in all three tests.

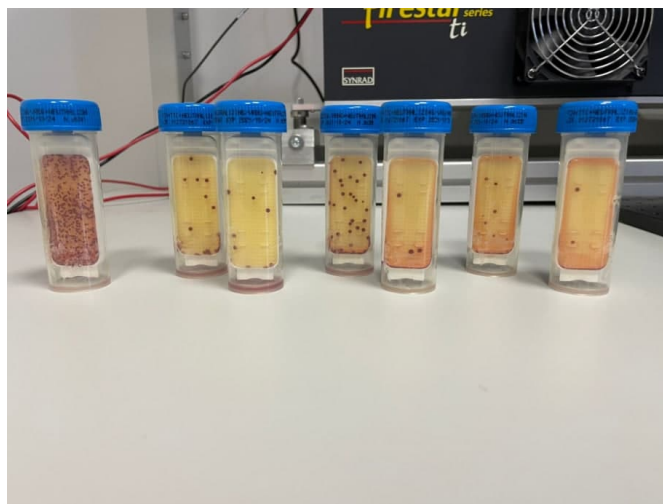


Figure 6.5: Post-exposure: experiments with 2 s, 20 mL of contaminated water.

6.1.4 Third set of tests

In order to demonstrate the repeatability of the previous results, have been used both the concentrations of the previous experiment and the same irradiation time.

Results

Observing Figure 6.6, the test tubes are arranged in the following way: on the left there is the control sample, followed by the pair of 2 s tests, in particular, the front test tubes are related to UVC irradiations only, while the rear ones are related to irradiations generated by the combination of both LEDs. It can be seen that the test has been partially successful, starting from a high concentration of *Eterobacteriaceae* (approx. 10^5 CFU/mL) a concentration of maximum 10^2 – 10^3 CFU/mL on the agar surfaces is obtained.

Besides, in a couple of test tubes the presence of colonies is not very noticeable, but it can be observed how the bacteria have grown on the lower part of the agar surface: surely, the agar has lost some liquid and due to the gravity the bacteria have accumulated in the lower part of the agar.

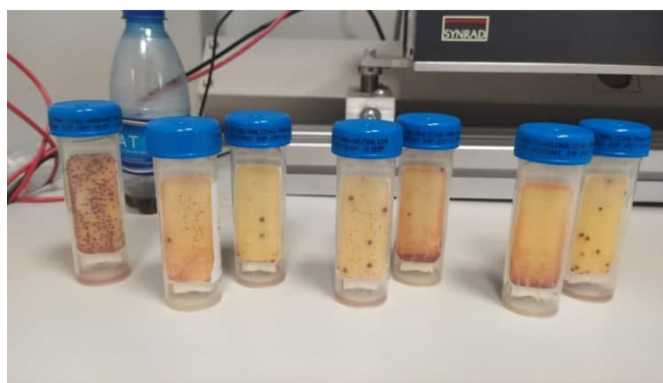


Figure 6.6: Post-exposure: experiments with 2 s, 20 mL of contaminated water.

6.1.5 Discussion

This first experimental part carried out comparing the two UVC and blue sources for disinfection of contaminated water with *Enterobacteriaceae* has shown positive results about the synergistic action of the two. Although the germicidal action of UVC-LEDs is more damaging at longer exposure times (3-5 s), coupling it with 405 nm radiation at lowest irradiation times (2 s) has brought an increase in antimicrobial power, although if with lesser contributions: starting from a bacterial concentration of 10^5 CFU/mL it is possible to achieve a reduction of 10^2 – 10^3 CFU/mL, thanks to the contribution of both.

6.2 Experimental Section 2: UVC-LEDs in aluminum tube

This second experimental part is focused on the use of only UVC-LED sources (275 nm) for water disinfection, due to its limited exposure times and stronger germicidal effect: a likely situation of a sanitizing system of hydraulic pipes has been simulated with a square base aluminum tube structure. Aluminum has been selected because, as demonstrated before, its reflection is able to improve the radiant energy field inside the tube, acting as a mirror for the incident UV-rays. Tests have been conducted always analyzing samples containing *Enterobacteriaceae* dissolved in water.

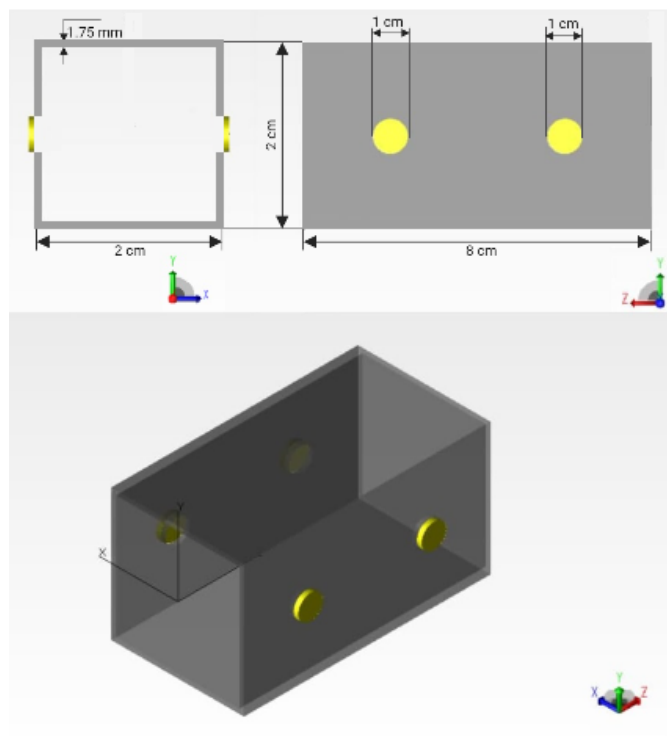


Figure 6.7: Simulated aluminum tube with *TracePro*.

Initial considerations

A demonstrator consisting of a hollow square section aluminum tube with an inner side of 1.7 cm, wall thickness of 1.5 mm and length of 8 cm has been physically realized and the simple representation on *TracePro* is reported in Fig. 6.7. On the length of the tube, on two parallel sides, 4 holes has been drilled on each side at

a distance of 4 cm between them, on which were applied quartz windows with a thickness of 3 mm. The overall UV absorption within quartz is small [40] and the quartz window allows the positioning of the 4 LEDs and would be in direct contact with water, protecting the sources from corrosion. Each LED emits at 275 nm with optical power of 100 mW. The demonstrator will be crossed by the solution to be sanitized.

Two simple simulations have been done using *TracePro*: the contribution of water has not been considered. The first is about the mean incident irradiance on an horizontal plane (assumed as perfect transmitter) along the x-axis (Fig. 6.8): in the right side there is a representation of the smoothing plot of the delivered irradiance from the 4 LEDs; it can be seen that the maximum values are only in proximity to the sources, confirming the previous studies. Whereas, the second simulation has been made evaluating the mean incident irradiance on a vertical plane (assumed as perfect transmitter) along the y-axis (Fig. 6.9): the right figure shows a more homogeneous irradiance distribution. It has been chosen the mean irradiance of the second configuration, for initial consideration on time of sanitization. Taking into account the selected disinfection threshold for *Enterobacteriaceae* of 6.6 mJ/cm^2 , the resulting mean irradiance of 25.75 mW/cm^2 needs 0.25 s to reach the 99% of bacterial disinfection.

Nevertheless, since the central part receives less radiation, because, as already said, there is accumulated fluence near the sources, the water flow that should invest the internal structure should be altered to allow a mixing of water and a consequent likelihood that a more homogeneous disinfection is provided to the entire volume of liquid [41].

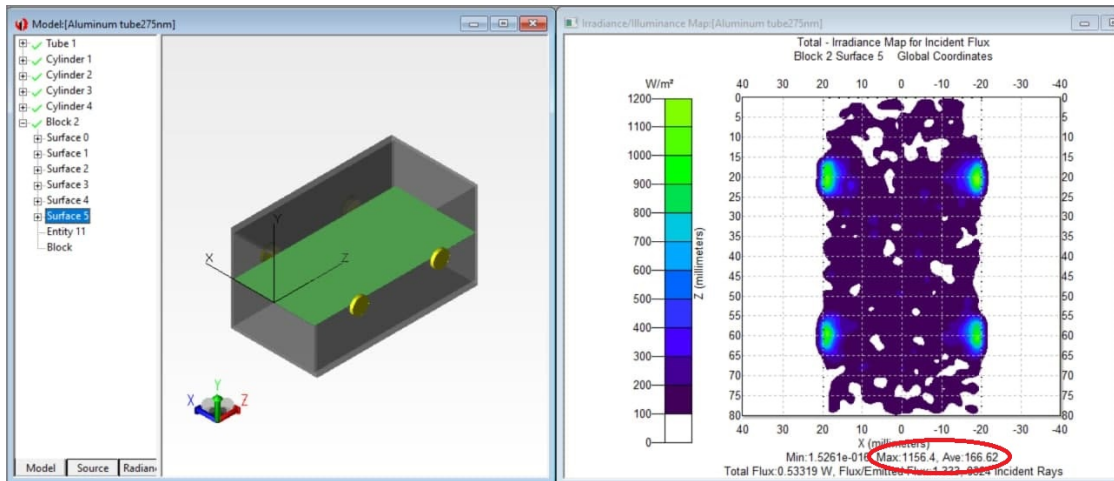


Figure 6.8: Irradiance simulation on a horizontal plane in the middle of the aluminum tube with *TracePro*.

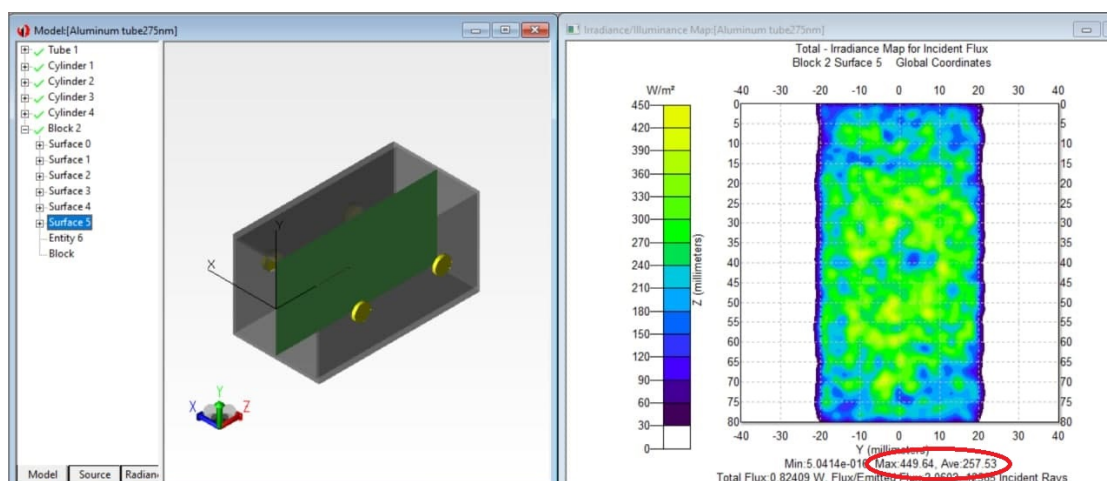


Figure 6.9: Irradiance simulation on a vertical plane in the middle of the aluminum tube with *TracePro*.

6.2.1 Material & Methods

Material used for irradiation

The employed instrumentation for these sets of experiments are: the aluminum tube, with the ends connected to two transparent plastic tubes, 12 mm, a DC 12 V submersible Pump with a flow rate of 10 L/min ($166.67 \text{ cm}^3/\text{s}$), two vessels for water collection and three *Contact Slide 1* tubes. The power supply is at 24 V and the incubator *IVYX Scientific* set at a temperature of 37 °C.

Methods

The test solution is obtained with the same process of the described experiments and the set-up is showed in Fig. 6.10. For these tests, the solution is initially contained in the first vessel and, after passing through the sanitizing system, it has been collected in the second vessel. Subsequently, the sanitized fluid has been passed through the circuit again to be sanitized a second time. The concentration of *Enterobacteriaceae* has been evaluated before sanitization, after the first, and finally, after the second sanitization.

- **Step 1.** The immersion pump has been inserted in the first vessel, containing the solution to be sanitized. One end of the demonstrator is connected to the pump through one of the two rubber tubes, while the other end is connected to the other rubber tube, which conveys it to the collecting vessel. The first “*Check*” test tube has been immersed into the starting solution for 7 s and the pumping system has been activated, keeping the LEDs active until the liquid

in the container was exhausted (the pump has been activated 10 s after the LEDs stabilization). Then a second “*Sterilization 1*” tube has been inserted into the collection vessel for 7 s.

- **Step 2.** In the second phase of testing, the sterilized solution has been employed as a starting solution, to be sanitized in the second cycle. The procedure is the same as described for the first step. At the end of the cycle the third test tube “*Sterilization 2*” has been inserted into the collection vessel for 7 s.
- **Step 3.** The 3 tubes have been kept at 37 °C for 24 h in the incubator.

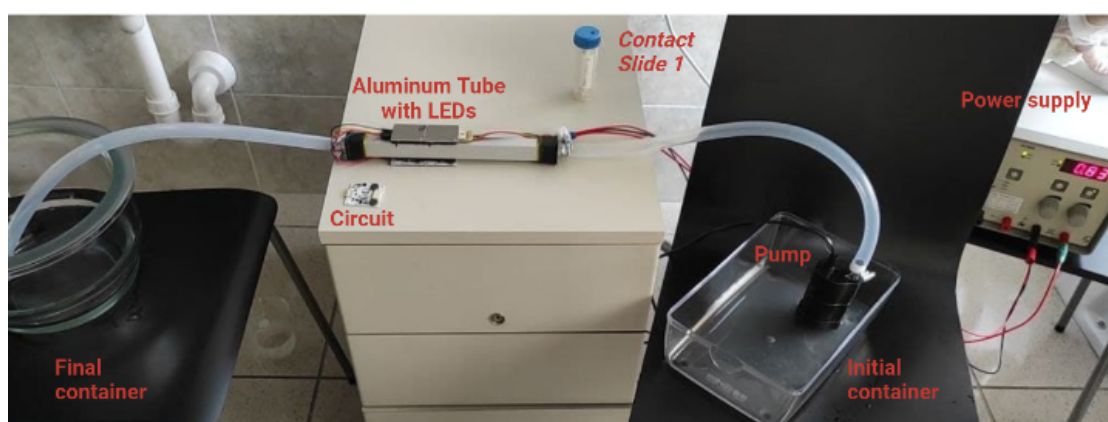


Figure 6.10: Set-up for the Experimental Section 2.

6.2.2 First set of tests

The purpose of the tests carried out is to evaluate the sanitization of water flowing through the demonstrator described above.

Data of the experiment

The concentration of sample of bacteria is 40 mL (feline feces) dissolved in a beaker containing approximately 500 mL of purified water.

Results

After the 24 h of incubation, the results are those in Fig. 6.11. On the agar of the “*Check*” tube, the first on the left, a number of bacterial colonies lower than

10^3 CFU/mL has been detected. After the first phase, a reduction of 70.5% on the “*Sterilization1*” tube, the middle one, has been seen, while after the second phase, on the “*Sterilization1*” tube, the rightmost one, a decrease in the concentration of the bacterial load of 94.1% has been evaluated, indicating a positive outcome of the sterilization treatment carried out.

Although the results are largely acceptable, the complete sanitization of the solution has not been achieved, perhaps due to the low quantity of water used, which, inside the system, created bubbles and has a turbulent flow, thus including the disadvantageous contribution of air.

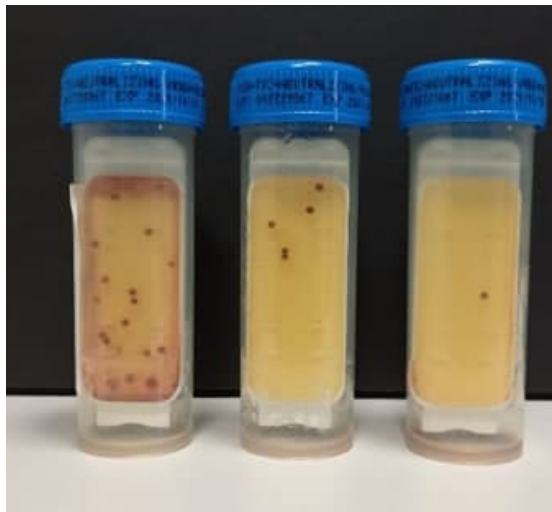


Figure 6.11: Post-exposure: 1st set of tests on aluminum tube.

6.2.3 Second set of tests

Data of the experiment

In this second set of experiments on the aluminum tube a difference is in the contaminated water used: a quantity of 1.5 L of water from the Po River has been sampled and the purposes are to test the river contamination and sanitize it with the designed structure. In addition, compared to the previous time, the amount of employed water is higher to avoid the turbulent phenomenon involving perhaps the air and try to achieve better results.

Results

The resulting agar after incubation are the following (Fig. 6.12). On the “*Check*” a quantity of 10^4 CFU/mL bacterial colonies has been identified, so the first result

obtained verifies the actual presence of *Enterobacteriaceae* in the water of the Po river, allowing its use in future applications. From the test tube “Sterilization1” the bacterial presence after the treatment has been decreased by about 10^2 CFU/mL and reduced almost completely during the second phase of the experiment. This result can be attributed to the use of an adequate amount of water that prevents the formation of turbulent flow and air bubbles in the system.



Figure 6.12: Post-exposure: 2nd set of tests on aluminum tube.

6.2.4 Discussion

In this second experimental part the metal tube system for sanitizing contaminated water was applied. Experiments conducted on bacteria from feline feces and Po river water have shown the presence of *Enterobacteriaceae* in both solutions.

Two subsequent sterilizations of the same water have been subjected to the light treatment: the results are really positive, starting from a bacterial concentration of 10^4 CFU/mL, almost the total reduction has been achieved: this means that the number of used LEDs and the flow rate were adequate. However, in none of the two cases a decrease of 100% has been obtained: the reason should be found both in the flow dynamics and in the presence of reflection and absorption phenomena due to water and air bubbles. In fact, having used a greater quantity of water in the second case has allowed a more laminar flow (visual observation through the plastic tubes) that has favored more sterilization.

Future developments may include the insertion, inside the tube, of a small structure that can act as a mixer, to allow the entire volume of incoming water to reach the walls of the tube, where it is estimated to be the maximum irradiance.

6.3 Evaluations on Aluminum Tube

The configuration of 2-2 LEDs with the aluminum tube has been chosen for the further evaluations. It has been selected a reference dose of 6.6 mJ/cm^2 and the mean irradiance (E_{mean}) has been calculated at 1 cm for every simulation. The following are comparisons of the changing useful parameters to guarantee a sufficient germicidal action, using four LEDs of 30 mW, 50 mW, 100 mW and 500 mW. It has been decided to assess how vary: time exposure (t_{exp}), permitted length of the tube (l_{tube}), number of LEDs and associated costs as the flow rate of water inside the pipe and pipe diameter. The following average LED costs have been taken as reference values for cost calculations: 25 € for a 30 mW LED, 60 € for a 50 mW LED and 90 € for a 100 mW LED; since 500 LEDs are not even commercially available yet, it is not possible to provide an indicative cost.

Water flow rate: Q1 = 600 L/h

In Tables 6.1, 6.2, 6.3, 6.4, the flow rate has been held constant at $Q1 = 600 \text{ L/h}$ and the various situations associated with the use of pipes with diameters of $d1 = 1.7 \text{ cm}$, $d2 = 2.5 \text{ cm}$ (1 inch), $d3 = 5.08 \text{ cm}$ (2 inch), $d4 = 7.62 \text{ cm}$ (3 inch), respectively, are analyzed.

Table 6.1: Comparisons: $Q1 = 600 \text{ L/h}$, $d1 = 1.7 \text{ cm}$.

Radiant power	E_{mean} (mW/cm ²)	t_{exp} (s)	l_{tube} (cm)	N°LEDs	Cost (€)
30 mW	8.9	0.7	43	14	350
50 mW	14.9	0.4	26	9	540
100 mW	29.8	0.2	13	4	360
500 mW	149.4	0.04	2.5	1	?

Table 6.2: Comparisons: $Q1 = 600 \text{ L/h}$, $d2 = 2.5 \text{ cm}$.

Radiant power	E_{mean} (mW/cm ²)	t_{exp} (s)	l_{tube} (cm)	N°LEDs	Cost (€)
30 mW	6.0	1.1	30	10	250
50 mW	10.1	0.7	17.7	6	360
100 mW	20.1	0.3	9	3	270
500 mW	100.4	0.06	1.7	1	?

Table 6.3: Comparisons: $Q1 = 600 \text{ L/h}$, $d3 = 5.08 \text{ cm}$.

Radiant power	E_{mean} (mW/cm ²)	t_{exp} (s)	l_{tube} (cm)	N°LEDs	Cost (€)
30 mW	1.6	4.23	27	9	225
50 mW	2.6	2.5	16	5	300
100 mW	5.2	1.3	8	3	270
500 mW	26.2	0.2	1.6	1	?

Table 6.4: Comparisons: $Q1 = 600 \text{ L/h}$, $d4 = 7.62 \text{ cm}$.

Radiant power	E_{mean} (mW/cm ²)	t_{exp} (s)	l_{tube} (cm)	N°LEDs	Cost (€)
30 mW	0.7	9.4	27	9	225
50 mW	1.2	5.6	16.2	5	300
100 mW	2.3	2.8	8	3	270
500 mW	11.8	0.5	1.6	1	?

Water flow rate: $Q2 = 2,200 \text{ L/h}$

In Tables 6.5, 6.6, 6.7 and 6.8, instead, the same comparisons have been done with the second water flow rate of $2,200 \text{ L/h}$.

Table 6.5: Comparisons: $Q_2 = 2,200$ L/h, $d_1 = 1.7$ cm.

Radiant power	E_{mean} (mW/cm ²)	t_{exp} (s)	l_{tube} (cm)	N°LEDs	Cost (€)
30 mW	8.9	0.7	113	38	950
50 mW	14.9	0.4	68	23	1380
100 mW	29.8	0.2	34	11	990
500 mW	149.4	0.04	7	2	?

Table 6.6: Comparisons: $Q_2 = 2,200$ L/h, $d_2 = 2.5$ cm.

Radiant power	E_{mean} (mW/cm ²)	t_{exp} (s)	l_{tube} (cm)	N°LEDs	Cost (€)
30 mW	6.0	1.1	108	36	900
50 mW	10.1	0.7	65	22	1320
100 mW	20.1	0.3	32	11	990
500 mW	100.4	0.06	6	2	?

Table 6.7: Comparisons: $Q_2 = 2,200$ L/h, $d_3 = 5.08$ cm.

Radiant power	E_{mean} (mW/cm ²)	t_{exp} (s)	l_{tube} (cm)	N°LEDs	Cost (€)
30 mW	1.6	4.23	100	33	825
50 mW	2.6	2.5	60	20	1200
100 mW	5.2	1.3	30	10	900
500 mW	26.2	0.2	6	2	?

Table 6.8: Comparisons: $Q_2 = 2,200$ L/h, $d_4 = 7.62$ cm.

Radiant power	E_{mean} (mW/cm ²)	t_{exp} (s)	l_{tube} (cm)	N°LEDs	Cost (€)
30 mW	0.7	9.4	99	33	825
50 mW	1.2	5.6	60	20	1200
100 mW	2.3	2.8	30	10	900
500 mW	11.8	0.5	6	2	?

Chapter 7

Experimental Section 2 : Blue LED with curcumin for water disinfection

7.1 Blue light LED with curcumin on water

The second experimental part of the thesis work is about PDT and the coupling of a natural photosensitizer, curcumin, with a blue light source of 405 nm. The main purpose of these experiments is to test the real efficacy in order to design an alternative sanitization system; the bacterial compound of (*Enterobacteriaceae*) has been observed before and after the treatment. The same amount of curcumin has been involved for each trial in different forms like powdered, mixed with vinyl glue or with hardening resin and allowed to solidify. Vinyl glue and resin have been selected for their transparency: it was thought that a solid but transparent compound that could facilitate the splitting of curcumin molecules in reactive substances able to react with the surrounding bacteria and to cause their death.

7.2 Circuit: blue LED

The circuit used is the same as the previous experiments and only the blue LED (405 nm) has been connected in order to evaluate its antimicrobial action.

Initial considerations

It is well known that blue-light has extremely lower disinfection properties than UVC sources. Referring to Figure 6.1 (right), the averaged irradiance for the blue-source is 68 mJ/cm^2 and considering that the required dose for 99% inactivation of *E. coli* is of 108 J/cm^2 , it means that the exposure time should be of almost 26 minutes. Nonetheless, lower irradiation time in examined tests have been applied because it has been intended to experiment the various behaviors of the different forms of PS used, as the dynamics of action of this coupling is not yet well known, and then proceed in future studies with the use of the best composition with longer exposure times.

7.2.1 Material & Methods

Material used for irradiation

The instrumentation for this experimental part consist in: blue-LED source (405 nm) of 2.4 W of optical power, the power supply is at 24 V, *Contact Slide 1*, Liofilchem®, the agar culture medium for *Enterobacteriaceae*, the incubator *IVYX Scientific* at 37°C , multi-well Petri dishes, steryliized syringes and curcumin. The set-up for these experiments is in Figure 7.1: the LED source is positioned at a distance of 2.5 cm from the ground and multi-well Petri dishes, with water to sanitize have been put under it, trying to minimize the distance in order to improve the sterilization.

Curcumin samples

Six type of samples have been used, which are in the form of disk (of 35 mm diameter), pieces and powder (Fig. 7.2):

1. Disk of white vinyl glue (12 mL of vinyl glue added to 1.5 mL of water);
2. Disk of vinyl glue and curcumin with curcumin powder on the surface (12 mL of vinyl glue added to 1.5 mL of water and plus a curcumin teaspoon and some curcumin powder has been sprinkled on the surface during the drying process);
3. Disk of mixed vinyl glue and curcumin (12 mL of vinyl glue added to 1.5 mL of water and plus a curcumin teaspoon);
4. Thick pieces of vinyl glue and curcumin mixed, made using the same previous quantities of vinyl glue and curcumin, made from a solid cube left to dry for several days;
5. Disk of mixed resin and curcumin, *Norland Optical Adhesive 61*, a resin with improved water resistance, which cures with a UV lamp;

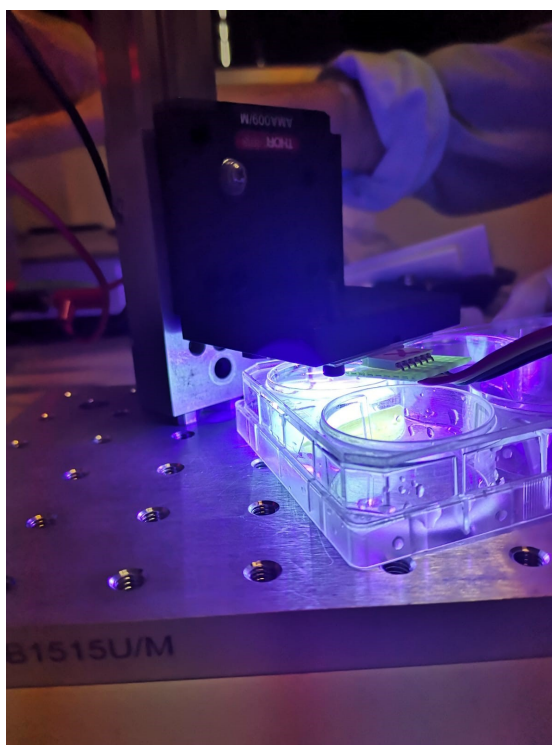


Figure 7.1: Set-up for blue-LED experiments.

6. Powder curcumin.

Methods

The same steps explained in *Section 6.1.1* and represented in Figure 6.3 have been executed for this set of tests: it aims at verifying the disinfectant action of curcumin with blue light. The supply voltage is 24 V and the blue LED is previously turned on and stabilized for 10 seconds. Each well of the Petri dish is filled with contaminated water (from the Po River) by means of a sterilized syringe, the disks/curcumin powder, according to the type of test to be performed, has been inserted inside; the content is irradiated with the blue LED placed at 2.5 cm distance for a time equal to 1 minute and then, with the help of the second syringe, the treated solution is withdrawn to impregnate the test tubes *Contact Slide 1*.

7.2.2 First set of tests

An initial evaluation of irradiation times and reactions of the various PS potential samples immersed in water with the incident blue light has been performed.

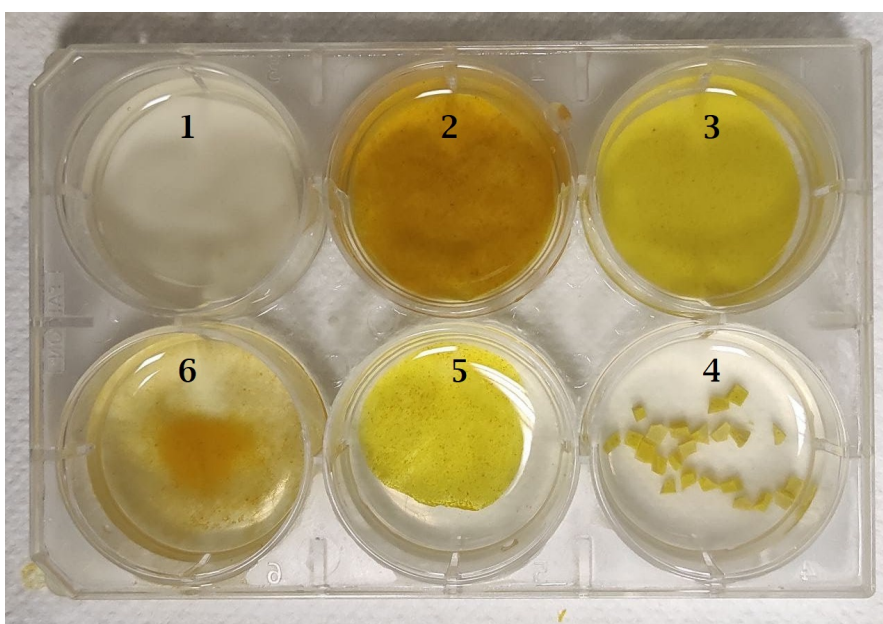


Figure 7.2: Curcumin samples: 1) disk of white vinyl glue, 2) vinyl glue and curcumin disc with curcumin powder on the surface, 3) disk of mixed vinyl glue and curcumin, 4) thick pieces of vinyl glue and curcumin mixed, 5) disk of mixed resin and curcumin, 6) curcumin powder.

Data of experiment

For this set of tests 14 culture medium slides have been used for the following 14 different experiments (“C-W” stands for contaminated water and “BL” for blue-light):

1. C-W (test);
2. C-W + BL (1 min);
3. C-W + powder curcumin;
4. C-W + powder curcumin + BL (1 min);
5. C-W + powder curcumin + BL (2 min);
6. C-W + white vinyl glue disk;
7. C-W + white vinyl glue disk + BL (1 min);
8. C-W + mixed vinyl glue and curcumin disk;
9. C-W + mixed vinyl glue and curcumin disk + BL (1 min);

10. C-W + mixed vinyl glue and curcumin disk + BL (2 min);
11. C-W + mixed vinyl glue and curcumin disk with curcumin powder on surface;
12. C-W + mixed vinyl glue and curcumin disk with curcumin powder on surface + BL (1 min);
13. C-w + pieces of mixed vinyl glue and curcumin;
14. C-w + pieces of mixed vinyl glue and curcumin + BL (1 min);
15. C-W + resin and curcumin disk;
16. C-W + resin and curcumin disk + BL (1 min).

Results

After the 24 h of incubation at 37°C, on the agar of the slides have emerged the following results (Fig. 7.3):



Figure 7.3: Tests 1-16.

The best results have been obtained for those tests carried out for longer exposure

times (Test 5 and 10). In general, curcumin powder seems to be more efficient than the solid vinyl glue of the Test 10: even if it is not clear if results from Test 10 are due to the effectiveness of the disinfection or if, due to gravity, the bacteria have leaked to the bottom of the tube, it can be said that the powder curcumin has showed better performances, perhaps because curcumin molecules, not being held in any layer of different material, come into contact with blue light more easily, creating the unstable radicals faster which could be responsible for the success of the experiment.

Finally, at the end of the treatment, all disks, except those composed of resin + curcumin, flake in water and this does not make them fully integrable in a future system of disinfection (Fig. 7.4).

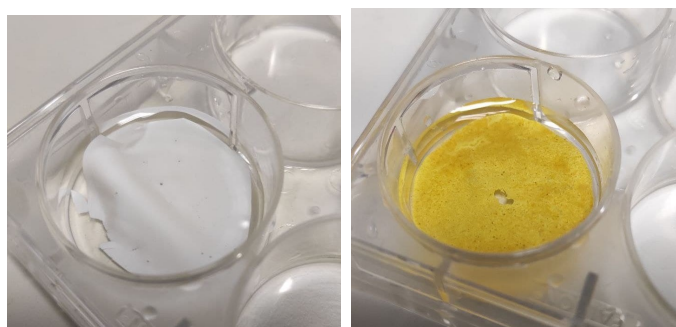


Figure 7.4: Post irradiation vinyl glue disks residues.

7.2.3 Second set of tests

In the previous experiments, curcumin powder and vinyl glue disk with curcumin have demonstrated better performance, thus tests have been repeated by simply lengthening the exposure times and evaluating their behavior.

Data of experiments

Each test has been performed in a different well of the Petri dish: inside it has been placed the vinyl glue disc with curcumin or dissolved curcumin powder and then it has been filled with the contaminated fluid. In both cases the contents have been left to stand for 3 minutes and then irradiated. This choice has been made in order to understand if the samples, in contact for more time with curcumin undergo changes or not. Seven *Contact Slide 1* have been used for the bacterial detection of the tests (“C-W” stands for contaminated water and “BL” for blue-light):

1. C-W (test), “Check”;
2. C-W + vinyl glue and curcumin disk + BL (1 min);
3. C-W + vinyl glue and curcumin disk + BL (3 min);
4. C-W + vinyl glue and curcumin disk + BL (4 min);
5. C-W + powder curcumin + BL (1 min);
6. C-W + powder curcumin + BL (3 min);
7. C-W + powder curcumin + BL (4 min);

Results

The tubes are then placed at 37 °C for 24 hours in an incubator and the results obtained are shown in Figure 7.5: it has emerged that by increasing the exposure time the disinfection effect is enhanced; moreover, curcumin powder dissolved in water continues to represent the most advantageous situation, although of poor application because of the yellowish color that it would leave in the solution.

The graphic below has been obtained with the segmentation of images of the agar medium culture after each test and the percentage reduction of each treatment compared to the initial bacterial concentration on “Check” (Test 1) has been calculated: the first three bar diagrams represent the curcumin powder tests (5-6-7) and the other three are those of the vinyl glue and curcumin disc tests (2-3-4) at 1, 3 and 4 minutes respectively.

It can be seen that the segmentation shows little reduction after 1 and 3 minutes of curcumin powder treatment, which increases rapidly in the 4 minute test; whereas,

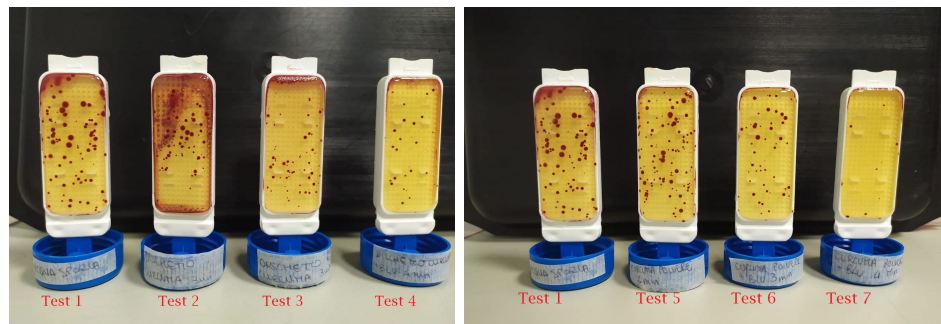


Figure 7.5: Tests 1-7.

for the disks, it seems that the 3 minute test results are much more advantageous than the respective with powder and the 4 minute test results are greater for the same class of test, but less than the previous one.

It would be advisable to keep repeating the tests, even making more attempts for the same type of test to verify the repeatability and reliability of the obtained results.

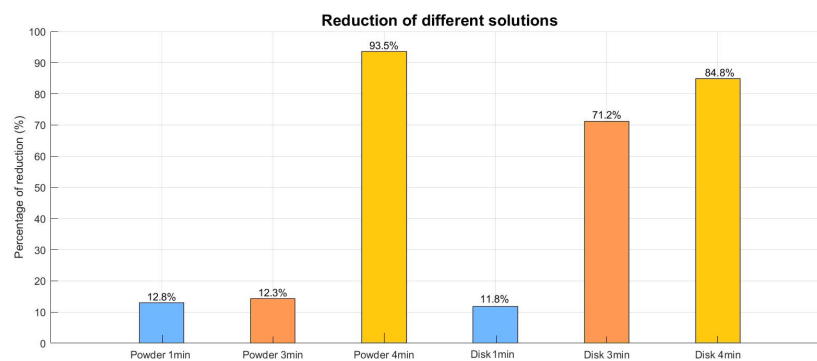


Figure 7.6: Reduction of different solutions of curcumin: powder curcumin and disk with glue and curcumin comparisons at different time exposure.

7.2.4 Discussion

It can be stated that in order to achieve the 93.5% of bacterial reduction through the use of Photo-Dynamic Therapy, with blue light and curcumin, it is necessary to provide radiation for at least 4 minutes. The photosensitizers in powder form allows obtaining the achieved high percentage of bacterial inactivation because it

is directly invested by radiation and this leads to release more quickly its cytotoxic radicals for the surrounding bacteria; in the solution with curcumin and glue disks, the situation is mostly similar, with a microbial reduction of 84.8%, less performing than the previous one, but still functioning. This result can be explained with the composition of the disk itself: the glue perhaps holds the produced radicals inside, preventing their partial escape and the complete functionality of the treatment. Both are therefore valid solutions, but they need to be improved in order to be integrated in a real disinfection system because, after irradiation, they have released residues in the treated liquid, that can affect the quality of the water. In addition, future studies should analyze different exposure times; different curcumin concentrations could be tested and new materials that provide a solid substrate but allowing the activation of curcumin reactions are recommended to be tried.

Chapter 8

Conclusions

In this Master's thesis work two light-based techniques for bacterial inactivation have been addressed: Ultra-Violet (200 nm to 280 nm) and blue light based Photo-Dynamic Therapy. Both of them are particularly interesting because, not being based on the use of antibiotics, do not contribute to the problem of antibiotic resistance. Moreover, they have also anti-viral actions and therefore can also contribute in limiting the SARS-CoV-2 infections.

UVC light antimicrobial mechanism relies on the direct damage of the pathogen DNA, while the PDT, exploiting the interaction of visible light with suitable photosensitizers, produces toxic reactive oxygen species that damage the cells.

This thesis work focused on the study of the simultaneous antimicrobial efficacy of UVC and blue light for water sanitization, one of the 17 topic addressed in the UN 2030 Sustainable Development Goals. UV and blue lights have been generated with LEDs, a choice that allowed overcoming the limitations of previously used low-pressure mercury lamps.

In the first part of this project a MATLAB® code has been developed to evaluate the distribution of the irradiance on a plane as a function of the number of LEDs and of their relative positions. The model is based on the simplification of considering each LED as a Lambertian source, but, when compared against a professional ray-tracing optical software, it turned out to be accurate enough for the intended application. Five LED geometries on a single or on two parallel planes have been analyzed, considering also impact of the reflectance from the metallic walls should the proposed system be used to disinfect water in pipe. The best configurations allow obtaining an uniform irradiance distribution high enough to guarantee an almost complete sterilization in just 0.07 s.

In the second part of the work, the efficacy on contaminated water of two simultaneous sources, UVC-LED (275 nm, 100 mW) and blue-LED (405 nm, 2.4 W) has been experimentally tested using with agar culture medium for the detection of *Enterobacteriaceae*. The result has been satisfactory: although it is known that

for long exposure times the UVC source is much more powerful than the blue one, for radiation times of 2 s the contribution of both sources have led to a bacterial decrease of 10^2 – 10^3 CFU/mL.

Some tests have been conducted also simulating a “sanitizing pipe” in which the disinfection action occurs as the contaminated water flows inside it. The results showed an almost 100% bacterial inactivation for usual tap water flow of about 10 L/min. Future studies could miniaturize the device and extend the effect on pipes with larger flows.

Finally, some tests have been carried out to study the efficacy of the combination of blue light with curcumin acting a photosensitizer. This a combination already demonstrating to work in other applications (for example, dentistry), but not applied to water before. Even if the release of yellow residues in the post-irradiation solution requires further studies to be fully applicable in a future sanitization system, the two best solutions that reported an inactivation after 4 minutes of 84.8 % and 93.5 % respectively, were those composed of curcumin and vinyl glue disc and curcumin powder. The latter composition allows a more quickly release of substances harmful to bacterial colonies because not retained in any solid matrix, but free to perform their proven antibacterial action in the samples to be sanitized.

Bibliography

- [1] Michael R Hamblin and Heidi Abrahamse. «Can light-based approaches overcome antimicrobial resistance?» In: *Drug development research* 80 (2019), pp. 48–67 (cit. on pp. 3, 22–25).
- [2] URL: <https://www.marionegri.it/magazine/citrobacter-verona+&cd=1&hl=it&ct=clnk&gl=it> (cit. on p. 5).
- [3] URL: <https://www.colormatters.com/color-and-science/electromagnetic-color> (cit. on p. 6).
- [4] M. Wegelin, Silvio Canonica, K. Mechsner, Thomas Fleischmann, F. Pesaro, and A. Metzler. «Solar water disinfection: Scope of the process and analysis of radiation experiments». In: *Aqua: Journal of Water Supply Research and Technology* 43 (Jan. 1994), pp. 154–169 (cit. on p. 10).
- [5] Maya B. Mane, Vinay M. Bhandari, and Vivek V. Ranade. «Safe water and technology initiative for water disinfection: Application of natural plant derived materials». In: *Journal of Water Process Engineering* 43 (2021), p. 102280 (cit. on p. 10).
- [6] Susan D Richardson and Cristina Postigo. «Drinking water disinfection by-products». In: *Emerging organic contaminants and human health*. Springer, 2011, pp. 93–137 (cit. on pp. 10–12).
- [7] W.B. Hugo. «A Brief History of Heat, Chemical and Radiation Preservation and Disinfection». In: *International Biodeterioration Biodegradation* 36, Issues 3–4 (Oct. 1995) (cit. on p. 10).
- [8] David Lytle and Jose-Luis Sagripanti. «Predicted inactivation of viruses of relevance to biodefense by solar radiation». In: *Journal of virology* 79 (Nov. 2005), pp. 14244–52 (cit. on p. 10).
- [9] Rui Yin, Tianhong Dai, Pinar Avci, Ana Elisa Serafim Jorge, Wanessa CMA de Melo, Daniela Vecchio, Ying-Ying Huang, Asheesh Gupta, and Michael R Hamblin. «Light based anti-infectives: ultraviolet C irradiation, photodynamic therapy, blue light, and beyond». In: *Current Opinion in Pharmacology* 13.5 (2013), pp. 731–762 (cit. on pp. 11, 24).

- [10] Do-Kyun Kim, Dong-Hyun Kang, and Christopher A. Elkins. «Elevated Inactivation Efficacy of a Pulsed UVC Light-Emitting Diode System for Foodborne Pathogens on Selective Media and Food Surfaces». In: *Applied and Environmental Microbiology* 84.20 (2018), e01340–18 (cit. on p. 11).
- [11] Paul Onkundi Nyangaresi, Yi Qin, Guolong Chen, Baoping Zhang, Yinghua Lu, and Liang Shen. «Comparison of the performance of pulsed and continuous UVC-LED irradiation in the inactivation of bacteria». In: *Water Research* 157 (2019), pp. 218–227 (cit. on pp. 13, 21).
- [12] Igor Shuryak David J. Brenner Manuela Buonanno David Welch. «Far-UVC light (222nm) efficiently and safely inactivates airborne human coronaviruses». In: *Scientific Reports* 10 (2020) (cit. on p. 13).
- [13] Shanthi Narla, Alexis B. Lyons, Indermeet Kohli, Angeli E. Torres, Angela Parks-Miller, David M. Ozog, Iltefat H. Hamzavi, and Henry W. Lim. «The importance of the minimum dosage necessary for UVC decontamination of N95 respirators during the COVID-19 pandemic». In: *Photodermatology, Photoimmunology & Photomedicine* 36.4 (2020), pp. 324–325 (cit. on p. 13).
- [14] Gilbert Held. *Introduction to light emitting diode technology and applications*. Auerbach publications, 2016 (cit. on pp. 13, 15).
- [15] URL: <https://www.colormatters.com/color-and-science/electromagnetic-color> (cit. on p. 15).
- [16] Do-kyun Kim and Dong-Hyun Kang. «Effect of surface characteristics on the bactericidal efficacy of UVC LEDs». In: *Food Control* 108 (2020), p. 106869 (cit. on p. 16).
- [17] Majid Keshavarzfathy and Fariborz Taghipour. «Computational modeling of ultraviolet light-emitting diode (UV-LED) reactor for water treatment». In: *Water Research* 166 (2019), p. 115022 (cit. on pp. 16, 17).
- [18] Sunday S Nunayon, Huihui Zhang, and Alvin CK Lai. «Comparison of disinfection performance of UVC-LED and conventional upper-room UVGI systems». In: *Indoor Air* 30.1 (2020), pp. 180–191 (cit. on p. 16).
- [19] URL: <https://www.mcknightsseniorliving.com/home/columns/mark-etplace-columns/the-science-behind-uvc-light-and-why-its-critical-for-senior-living-community-safety> (cit. on p. 17).
- [20] Qiqi Wan, Gang Wen, Ruihua Cao, Xiangqian Xu, Hui Zhao, Kai Li, Jingyi Wang, and Tinglin Huang. «Comparison of UV-LEDs and LPUV on inactivation and subsequent reactivation of waterborne fungal spores». In: *Water Research* 173 (2020), p. 115553 (cit. on p. 18).

- [21] Surapong Rattanakul and Kumiko Oguma. «Inactivation kinetics and efficiencies of UV-LEDs against *Pseudomonas aeruginosa*, *Legionella pneumophila*, and surrogate microorganisms». In: *Water Research* 130 (2018), pp. 31–37 (cit. on p. 18).
- [22] Christie Chatterley. «UV-LED Irradiation Technology for Point-of-Use Water Disinfection». In: *Proceedings of the Water Environment Federation 2009* (Jan. 2009) (cit. on p. 18).
- [23] Colleen Bowker, Amanda Sain, Max Shatalov, and Joel Ducoste. «Microbial UV fluence-response assessment using a novel UV-LED collimated beam system». In: *Water research* 45.5 (2011) (cit. on p. 19).
- [24] Rui Yin, Tianhong Dai, Pinar Avci, Ana Elisa Serafim Jorge, Wanessa CMA de Melo, Daniela Vecchio, Ying-Ying Huang, Asheesh Gupta, and Michael R Hamblin. «Light based anti-infectives: ultraviolet C irradiation, photodynamic therapy, blue light, and beyond». In: *Current opinion in pharmacology* 13.5 (2013), pp. 731–762 (cit. on pp. 19, 20, 25).
- [25] Do-Kyun Kim, Soo-Ji Kim, and Dong-Hyun Kang. «Bactericidal effect of 266 to 279 nm wavelength UVC-LEDs for inactivation of Gram positive and Gram negative foodborne pathogenic bacteria and yeasts». In: *Food Research International* 97 (Apr. 2017) (cit. on p. 20).
- [26] Dana Pousty, Ron Hofmann, Yoram Gerchman, and Hadas Mamane. «Wavelength dependent time–dose reciprocity and stress mechanism for UV-LED disinfection of *Escherichia coli*». In: *Journal of Photochemistry and Photobiology B: Biology* 217 (2021), p. 112129 (cit. on p. 20).
- [27] Sara E Beck, Natalie M Hull, Christopher Poepping, and Karl G Linden. «Wavelength-dependent damage to adenoviral proteins across the germicidal UV spectrum». In: *Environmental science & technology* 52.1 (2018), pp. 223–229 (cit. on p. 20).
- [28] Do-Kyun Kim, Dong-Hyun Kang, and Christopher A. Elkins. «Elevated Inactivation Efficacy of a Pulsed UVC Light-Emitting Diode System for Foodborne Pathogens on Selective Media and Food Surfaces». In: *Applied and Environmental Microbiology* 84.20 (2018), e01340–18 (cit. on p. 21).
- [29] Hassan Mahmoudi, Abbas Bahador, Maryam Pourhajibagher, and Mohammad Yousef Alikhani. «Antimicrobial photodynamic therapy: an effective alternative approach to control bacterial infections». In: *Journal of lasers in medical sciences* 9.3 (2018), p. 154 (cit. on pp. 22, 24).
- [30] Cindy Shehatou, Stephan L Logunov, Paul M Dunman, Constantine G Haidaris, and W Spencer Klubben. «Characterizing the antimicrobial properties of 405 nm light and the Corning® light-diffusing fiber delivery system». In: *Lasers in surgery and medicine* 51.10 (2019), pp. 887–896 (cit. on p. 25).

- [31] Schmid, Katharina Hönes, Petra Vatter, and Martin Hessling. «Antimicrobial Effect of Visible Light—Photoinactivation of *Legionella rubrilucens* by Irradiation at 450, 470, and 620 nm». In: *Antibiotics* 8 (Oct. 2019), p. 187 (cit. on p. 25).
- [32] Violet V Bumah, Daniela S Masson-Meyers, Susan Cashin, and Chukuka S Enwemeka. «Optimization of the antimicrobial effect of blue light on methicillin-resistant *Staphylococcus aureus* (MRSA) in vitro». In: *Lasers in surgery and medicine* 47.3 (2015), pp. 266–272 (cit. on p. 25).
- [33] Leon Leanse, Xiaojing Zeng, and Tianhong Dai. «Potentiated antimicrobial blue light killing of methicillin resistant *Staphylococcus aureus* by pyocyanin». In: *Journal of Photochemistry and Photobiology B Biology* 215 (Feb. 2021), p. 112109 (cit. on p. 25).
- [34] Elisabetta Merigo, Stefania Conti, Tecla Ciociola, Maddalena Manfredi, Paolo Vescovi, and Carlo Fornaini. «Antimicrobial Photodynamic Therapy Protocols on *Streptococcus mutans* with Different Combinations of Wavelengths and Photosensitizing Dyes». In: *Bioengineering* 6.2 (2019), p. 42 (cit. on p. 25).
- [35] Chukuka S. Enwemeka, Terrance L. Baker, and Violet V. Bumah. «The role of UV and blue light in photo-eradication of microorganisms». In: *Journal of Photochemistry and Photobiology* 8 (2021), p. 100064 (cit. on pp. 25, 26).
- [36] Daniela Santos Masson-Meyers, Violet Vakunseh Bumah, Chris Castel, Dawn Castel, and Chukuka Samuel Enwemeka. «Pulsed 450 nm blue light significantly inactivates *Propionibacterium acnes* more than continuous wave blue light». In: *Journal of Photochemistry and Photobiology B: Biology* 202 (2020), p. 111719 (cit. on p. 26).
- [37] Chukuka S Enwemeka, Violet V Bumah, and John L Mokili. «Pulsed blue light inactivates two strains of human coronavirus». In: *Journal of Photochemistry and Photobiology B: Biology* 222 (2021), p. 112282 (cit. on p. 26).
- [38] Martina Riva Guido Perrone. «Radiometry and considerations on UVC LED sources for disinfection». In: (May 2020) (cit. on p. 29).
- [39] URL: https://www.portaleagentifisici.it/fo_ro_artificiali_riflettanza_materiali.php?lg=IT (cit. on p. 54).
- [40] Majid Keshavarzfathy and Fariborz Taghipour. «Radiation modeling of ultraviolet light-emitting diode (UV-LED) for water treatment». In: *Journal of Photochemistry and Photobiology A: Chemistry* 377 (2019), pp. 58–66 (cit. on p. 65).
- [41] Majid Keshavarzfathy and Fariborz Taghipour. «Computational modeling of ultraviolet light-emitting diode (UV-LED) reactor for water treatment». In: *Water research* 166 (2019), p. 115022 (cit. on p. 65).